

# **GEOLOGIC MAP OF THE CENTER 7.5-MINUTE QUADRANGLE, JEFFERSON COUNTY, WASHINGTON**

---

by Michael Polenz, Harley O. Gordon,  
Ian J. Hubert, Trevor A. Contreras,  
Annette I. Patton, Gabriel Legorreta Paulín,  
and Recep Cakir

WASHINGTON  
DIVISION OF GEOLOGY  
AND EARTH RESOURCES  
Map Series 2014-02  
December 2014

*This geologic map was funded in part by the USGS  
National Cooperative Geologic Mapping Program,  
award no. G13AC00173*



WASHINGTON STATE DEPARTMENT OF  
**Natural Resources**  
Peter Goldmark - Commissioner of Public Lands

## DISCLAIMER

Neither the State of Washington, nor any agency thereof, nor any of their employees, makes any warranty, express or implied, or assumes any legal liability or responsibility for the accuracy, completeness, or usefulness of any information, apparatus, product, or process disclosed, or represents that its use would not infringe privately owned rights. Reference herein to any specific commercial product, process, or service by trade name, trademark, manufacturer, or otherwise, does not necessarily constitute or imply its endorsement, recommendation, or favoring by the State of Washington or any agency thereof. The views and opinions of authors expressed herein do not necessarily state or reflect those of the State of Washington or any agency thereof.

This map product has been subjected to an iterative internal review process by agency geologists, cartographers, and editors and meets Map Series standards as defined by Washington Division of Geology and Earth Resources.

## INDEMNIFICATION

Research supported by the U.S. Geological Survey, National Cooperative Geologic Mapping Program, under USGS award number G13AC00173. The views and conclusions contained in this document are those of the authors and should not be interpreted as necessarily representing the official policies, either expressed or implied, of the U.S. Government.

## WASHINGTON STATE DEPARTMENT OF NATURAL RESOURCES

Peter Goldmark—*Commissioner of Public Lands*

## DIVISION OF GEOLOGY AND EARTH RESOURCES

David K. Norman—*State Geologist*

John P. Bromley—*Assistant State Geologist*

### Washington State Department of Natural Resources Division of Geology and Earth Resources

*Mailing Address:*

MS 47007  
Olympia, WA 98504-7007

*Street Address:*

Natural Resources Bldg, Rm 148  
1111 Washington St SE  
Olympia, WA 98501

*Phone:* 360-902-1450

*Fax:* 360-902-1785

*E-mail:* [geology@dnr.wa.gov](mailto:geology@dnr.wa.gov)

*Website:* <http://www.dnr.wa.gov/geology>

*Publications List:*

[http://www.dnr.wa.gov/ResearchScience/Topics/  
GeologyPublicationsLibrary/Pages/pubs.aspx](http://www.dnr.wa.gov/ResearchScience/Topics/GeologyPublicationsLibrary/Pages/pubs.aspx)

*Washington Geology Library Searchable Catalog:*

[http://www.dnr.wa.gov/ResearchScience/Topics/  
GeologyPublicationsLibrary/Pages/washbib.aspx](http://www.dnr.wa.gov/ResearchScience/Topics/GeologyPublicationsLibrary/Pages/washbib.aspx)

*Washington State Geologic Information Portal:*

<http://www.dnr.wa.gov/geologyportal>

*Suggested Citation:* Polenz, Michael; Gordon, H. O.; Hubert, I. J.; Contreras, T. A.; Patton, A. I.; Legorreta Paulin, Gabriel; Recep Cakir, 2014, Geologic map of the Center 7.5-minute quadrangle, Jefferson County, Washington: Washington Division of Geology and Earth Resources Map Series 2014-02, 1 sheet, scale 1:24,000, 35 p. text.

© 2014 Washington Division of Geology and Earth Resources  
Published in the United States of America

## Contents

Introduction .....	1
Geologic Overview .....	1
Bedrock .....	1
Quaternary Deposits.....	2
Pre-Vashon Sediment.....	2
Vashon Drift.....	2
Post-glacial Deposits .....	2
Regional Structural Setting .....	3
Methods.....	3
Description of Map Units.....	4
Quaternary Unconsolidated Deposits .....	4
Holocene Nonglacial Deposits .....	4
Latest Pleistocene to Holocene Nonglacial Deposits .....	4
Pleistocene Glacial and Nonglacial Deposits .....	5
Vashon Drift of the Fraser Glaciation.....	5
Sediments Older than the Vashon Stade.....	7
Tertiary Sedimentary and Volcanic Bedrock.....	7
Lyre Formation (Middle Eocene) .....	9
Results, Findings, and Observations .....	11
Bedrock Stratigraphy and Paleontology .....	11
Ages of Quaternary Units .....	11
Glacial Lakes, Shorelines, and Everson Interstade Marine Incursion .....	14
Structure .....	15
Structural Interpretation of the Map Area.....	15
Faults .....	16
Other Structures.....	18
Evidence for Active Deformation.....	19
Seismicity .....	19
Acknowledgments.....	21
References Cited .....	21
Appendix A. New Radiocarbon and Luminescence Age Estimates .....	28
Appendix B. Crustal Earthquake Data.....	31

## FIGURES

Figure 1. Lineaments within the Center quadrangle.....	17
Figure 2. Inset of lineaments near the border of the Center and Uncas quadrangles .....	18
Figure 3. Three-dimensional rendering of earthquake locations beneath the Center quadrangle and vicinity .....	20
Figure B1. Earthquakes and focal mechanisms near the Center quadrangle.....	31

**TABLES**

Table A1. Radiocarbon age-control data from the map area.....28  
Table A2. Infrared and optically stimulated luminescence  
age-control results from the map area. ....29  
Table A3. Luminescence analytical data.....30  
Table B1. Crustal earthquakes with focal mechanisms in and near the map area. ....32

**MAP SHEET**

Geologic map of the Center 7.5-minute quadrangle, Jefferson County, Washington

Figure M1. Shaded relief map of regional structures

Figure M2. Total alkalis versus silica plot of igneous rocks

Table M1. Summary of new age estimates for the map area

Table M2. New whole-rock geochemical analyses for one basalt  
and eight andesite to dacite samples

---

# Geologic Map of the Center 7.5-minute Quadrangle, Jefferson County, Washington

by Michael Polenz<sup>1</sup>, Harley O. Gordon<sup>1</sup>, Ian J. Hubert<sup>1</sup>, Trevor A. Contreras<sup>1</sup>, Annette I. Patton<sup>1</sup>,  
Gabriel Legorreta Paulín<sup>2</sup>, Recep Cakir<sup>1</sup>

<sup>1</sup> Washington Division of  
Geology and Earth Resources  
MS 47007  
Olympia, WA 98504-7007

<sup>2</sup> Universidad Nacional Autónoma de México  
Instituto de Geografía  
Ciudad Universitaria, Del Coyoacán  
cp 04510, México, D.F.

## INTRODUCTION

This pamphlet provides unit descriptions, interpretations, and data for the geologic map of the Center 7.5-minute quadrangle in the Puget Lowland between Quilcene to the south and Chimacum and Port Discovery to the north—the Olympic Mountains are located just southwest of the quadrangle (map and Fig. M1 on map sheet). The Center geologic map is part of a systematic effort to develop 1:24,000-scale geologic coverage along all of Hood Canal, a region that is increasingly populated, militarily important, geologically active, and ecologically sensitive. Water resources are also becoming increasingly scarce in the quadrangle, and improved geologic mapping is needed for informed resource management. The need to map this area is underscored by the recent recognition of previously unknown faults in nearby quadrangles (Contreras and others, 2013, 2014; Polenz and others, 2013). Our map and cross sections revise and add detailed field observations and new geological analyses to previous mapping and studies (Allison, 1959; Hanson, 1976; Gayer, 1976; Grimstad and Carson, 1981; Spencer, 1984; Yount and Gower, 1991; Yount and others, 1993; Simonds and others, 2004; unpub. field notes of Kathryn Hanson, AMEC, and Robert Carson, Whitman College, 2013). We incorporate review of several hundred well and boring records, and geotechnical reports from multiple sources (Wash. State Dept. of Ecology; U.S. Geological Survey [USGS]; Wash. State Dept. of Transportation). We systematically reviewed lineaments (topographic, mainly in lidar-based images, and aeromagnetic) and analyzed focal mechanisms of earthquakes within the map area. Appendix A presents new radiocarbon and luminescence age estimates and Appendix B presents seismic data. Rock geochemistry data are reported on the map sheet.

## GEOLOGIC OVERVIEW

### Bedrock

Although most of the map area is covered by Quaternary sediment, Eocene volcanic and Eocene to Oligocene marine sedimentary rocks have been mapped in the Center quadrangle by prior studies at scales ranging from 1:24,000 to 1:250,000.

Several studies did not assign formal names to bedrock (Jillson, 1915; Gayer, 1976, 1977; Hanson, 1976, 1977; Grimstad and Carson, 1981; Simonds and others, 2004). All others except Weaver (1937) mapped basalt as early to middle Eocene Crescent Formation—the oldest unit recognized in the map area (Allison, 1959; Tabor and Cady, 1978; Gower, 1980; Spencer, 1984; Yount and Gower, 1991; Dragovich and others, 2002); Weaver (1937) mapped basalt as “Metchosin volcanics”. Allison (1959) divided the Crescent Formation into lower (Metchosin) and upper members, but more recent workers divided the formation into a volcanic facies and a sedimentary facies that is typically basaltic-lithic to calcareous (Tabor and Cady, 1978; Gower, 1980; Spencer, 1984; Yount and Gower, 1991).

Weaver (1937), Allison (1959), Tabor and Cady (1978), and Spencer (1984) used named units for all sedimentary rocks upsection of the Crescent Formation; other researchers did not classify the sedimentary rock in such detail (Dragovich and others, 2002; Simonds and others, 2004). Middle Eocene, mostly chert-dominated marine sedimentary rocks are primarily conglomerate but range to sandstone and were mapped as Lyre Formation

by Allison (1959), Tabor and Cady (1978), Gower (1980), Spencer (1984), and Yount and Gower (1991). Gower (1980) and Yount and Gower (1991) asserted that Lyre Formation cherty conglomerate is separated by an angular unconformity from up-section cherty conglomerate that they mapped separately (see unit Em<sub>21c</sub> and *Structural Interpretation of the Map Area*). Andesitic volcanic rocks were mapped as Lyre Formation by Tabor and Cady (1978) and Simonds and others (2004), but were mapped as separate units by Allison (1959), Gower (1980), Yount and Gower (1991), and Dragovich and others (2002). Spencer (1984) used an upward-fining section within the Lyre Formation to separate the sandstone of Snow Creek as a distinct upper sedimentary member with fossil fauna of Narizian age (middle to late Eocene age; see also McDougall, 2007). Spencer (1984) mapped siltstone upsection of the sandstone of Snow Creek as Eocene Townsend Shale. Tabor and Cady (1978) and Yount and Gower (1991) similarly recognized a regional fining-upward trend but mapped all (Tabor and Cady, 1978) or some (Yount and Gower, 1991) sandstone and overlying finer-grained sedimentary rocks as undivided Twin River formation. The Twin River formation was later formally redesignated the Twin River Group (Snively and others, 1978) and has not been recognized near the map area by recent workers mapping at 1:24,000 scale (Haeussler and others, 1999; Schasse and Slaughter, 2005; Tabor and others, 2011; Contreras and others, 2014). Correlation of rocks in the map area to Twin River Group members (Hoko River, Makah, and Pysht Formations) is now discouraged (Elizabeth Nesbitt, Univ. of Wash., written and oral commun., 2014). At least some workers have concluded that some sedimentary rocks in the map area—especially where dominantly fine-grained—may be as young as Oligocene age (Tabor and Cady, 1978; Yount and Gower, 1991; Dragovich and others, 2002; Simonds and others, 2004).

## Quaternary Deposits

### PRE-VASHON SEDIMENT

Unlike adjacent areas (Gayer, 1976; Hanson, 1976; Schasse and Slaughter, 2005; Tabor and others, 2011; Contreras and others, 2014), the map area did not provide us with compelling evidence of pre-Vashon sediment. Prior mappers interpreted some sediment below Vashon Till in the east half of the quadrangle as pre-Vashon (Gayer, 1976; Hanson, 1976; Grimstad and Carson, 1976), but our field observations, petrographic analyses, and new age-control data caused us to reassign most of these deposits to Vashon advance outwash. However, observation of apparently similar deposits interpreted as older and nonglacial south of the map area renders this assignment tentative where not clearly constrained by our age sites (see *Ages of Quaternary Units*). We tentatively identified possible pre-Vashon deposits (units Qc and Qpu) along the southern and western map boundaries and refer to prior mapping (Gayer, 1976; Schasse and Slaughter, 2005) in showing unit Qpu at the northeastern map corner.

### VASHON DRIFT

The modern landforms of fluted uplands and intervening troughs in the map area are largely a construct of the Fraser Glaciation, which we associate with marine oxygen-isotope stage 2 (MIS 2) (Morrison, 1991) and all Vashon Drift in the map area, consistent with prior work elsewhere in the Puget Lowland (Booth and others, 2004; Troost and Booth, 2008; Polenz and others, 2013). Deposition of proglacial advance outwash in the “great lowland fill” was followed by subglacial erosion and deposition of till (Booth, 1994, p. 695). The resulting subglacial landforms and deposits of outwash and till are the dominant surficial features within the map area. At the end of the glaciation, ice-dammed lakes and then marine waters filled the topographic troughs (Bretz, 1910, 1913; Thorson, 1981, 1989; Dethier and others, 1995; Booth and others, 2004). As the ice dam(s) in the northern Puget Lowland disintegrated, lake levels dropped in stages, leaving behind a series of progressively lower and younger relict shorelines at discrete elevations (Haugerud, 2009; Ralph Haugerud, USGS, oral commun., 2013; Polenz and others, 2012c, 2013). We include recessional lake and marine deposits in units Qgof, Qgos, and Qgod.

### POST-GLACIAL DEPOSITS

We separate post-glacial deposits into strictly Holocene units and those that span the latest Pleistocene to Holocene. The onset of the Holocene (USGS Geologic Names Committee, 2010) and the end of the Fraser Glaciation do not coincide in the Puget Lowland. Among the Pleistocene to Holocene units, most deposition probably occurred close to the end of the glaciation, although hillslope erosion and sediment deposition clearly continue in the modern environment (see *Ages of Quaternary Units*).

## Regional Structural Setting

The map area is in the Cascadia subduction zone forearc, where oblique convergence causes active structures to accommodate shortening (Johnson and others, 2004; McCaffrey and others, 2007). Within 10 mi of the map area, most mapped faults and prominent lineaments, other than fluting, strike northwest (Fig. M1). This regional fabric suggests that active structures in the map area respond to the same stress field as the northwest-striking, right-lateral and transpressional southern Whidbey Island fault zone to the north, northeast, and east of the map area (Johnson and others, 1996; Sherrod and others, 2008; Blakely and others, 2011) and the Dabob Bay fault zone to the south of the map area (Blakely and others, 2009; Polenz and others, 2013; Contreras and others, 2014). In contrast, we and prior workers show faults in the map area striking northeast and east (Fig. M1) (Gower, 1980; Gower and others, 1985; Yount and Gower, 1991). The discrepancy between the northwesterly alignment of most known active faults in the region and the northeast or east alignment of faults in the map area could indicate that structures in the map area are (1) relict features, (2) represent a locally divergent strain (and stress?) field, or (3) result from complex tectonics that remain unexplained. We do not show the Hood Canal fault because we found no evidence for it in the map area (see *Structure* below).

## METHODS

We identified units from field observations, geomorphic expression (including our interpretations of lidar by Puget Sound Lidar Consortium, 2002), thin section analyses, hundreds of well and boring records, geotechnical reports, geophysical data, prior geologic mapping, ‘T-sheet’ historical topographic surveys along coastlines by the U.S. Coast & Geodetic Survey (USCGS, 1870), soils maps by the U.S. Department of Agriculture (2009), and aerial orthophotos<sup>1</sup>. We used USGS Fact Sheet 2010-3059 for the geologic time scale (USGS, 2010) and the Udden-Wentworth scale (table 5 in Pettijohn, 1957) to classify unconsolidated sediment. We used LANDSAT satellite image analysis calibrated against our field observations to help identify surface sediment particle sizes and bedrock character to refine our unit boundaries. Edge mismatches with adjacent quadrangles are intentional and based on differences of interpretation from prior mapping.

We used clast counts, petrographic review of sand content, sedimentary attributes (such as paleocurrent indicators and textural changes), and field relations to determine sedimentary sources and infer the source area of glacial ice. We assumed that sediment consisting almost exclusively of sedimentary rocks and mafic volcanic rocks (basalt) was derived from proximal bedrock sources, including rocks exposed in the Olympic Mountains and Eocene to Oligocene volcanic and sedimentary rocks exposed in and near the map area. Most sediments within the map area additionally contain high-grade metamorphic and plutonic rocks that do not occur in nearby bedrock exposures. These ‘exotic’ lithologies include quartzite, rock types containing primarily plagioclase feldspar (diorite or gabbro), plutonic rocks containing quartz and (or) potassium feldspar (granite), and other lithologies exotic to the map area but found to the north in the Coast Mountains of British Columbia, the northwest Cascade Range of Washington, and the San Juan Islands. Their presence in sediments of the map area indicates southward transport due to Cordilleran ice sheet advances from the Coast Mountains of British Columbia—thus we assume that sediments that lack these far-traveled lithologies were derived from more local sources. We did not detect sediment mineral assemblages that deviate from the two above groupings (proximal vs. exotic), but note that Contreras and others (2013, 2014) interpreted some sand from the Quilcene quadrangle south of our map area as derived from Snoqualmie River basin sources to the east; they mainly cited potassium feldspar and monocrystalline quartz from granitic sources. Exposures of the stratigraphically highest drift were systematically attributed to the Puget lobe of the Cordilleran ice sheet during the Vashon Stade of the Fraser Glaciation (MIS 2) unless we had specific reason to map older drift.

Geochemical samples were analyzed by ALS<sup>2</sup>, radiocarbon samples by Beta Analytic, Inc.<sup>3</sup>, and luminescence samples by Shannon Mahan<sup>4</sup>. Sedimentary rock microfossil samples were prepared by Ellington and Associates, Inc.<sup>5</sup>, and luminescence samples by Shannon Mahan. Sedimentary rock microfossil samples were analyzed by E. Nesbitt<sup>6</sup>.

<sup>1</sup> Photo series, in order of frequency of our use: 2009 30-cm color; 2011 1-m color; 2011 3-ft infrared; 2003–2005 18-in. color; 1990–2000 3-ft black and white

<sup>2</sup> ALS, 2103 Dollarton Hwy, North Vancouver, BC V7H 0A7 Canada

<sup>3</sup> Beta Analytic, Inc., 4985 SW 74th Ct, Miami, FL 33155

<sup>4</sup> USGS, Box 25046, MS 974, Denver, CO 80225

<sup>5</sup> Ellington and Associates, Inc., 1414 Lumpkin Rd, Houston, TX 77043

<sup>6</sup> Elizabeth Nesbitt, Burke Museum, University of Washington, Seattle, WA 98195

## DESCRIPTION OF MAP UNITS

### Quaternary Unconsolidated Deposits

#### HOLOCENE NONGLACIAL DEPOSITS

- af Artificial fill**—Sand, cobbles, pebbles, boulders, silt, clay, organic matter, rip-rap, and concrete, in varied amounts, placed to elevate the land; engineered or non-engineered; shown where readily verifiable, fairly extensive, and thick enough (>5 ft) to be geotechnically significant; excludes roads and areas where underlying geology was deemed more informative. Unit **af** is manmade and therefore historic in age.
- Qb Beach deposits**—Sand, pebbles, pebbly sand, cobbles, silt, clay, shells, wood, peat, and isolated boulders; loose; clasts typically moderately to well rounded and oblate; locally well sorted; derived from shore bluffs, streams, and underlying deposits. Unit **Qb** is transient in the modern environment; episodic or periodic erosion at times exposes underlying units. The age of unit **Qb** is constrained to less than about 6,000 yr BP because before that time, sea level was too low to deposit beach sediment at or above present-day sea level (Eronen and others, 1987; Dragovich and others, 1994; Mosher and Hewitt, 2004).
- Qm Saltmarsh deposits**—Organic sediment and (or) loose clay, silt, and sand in a saltwater to brackish coastal wetland; identified only along the Port Discovery shore (sec. 19, T29N R1W), where a ‘T-sheet’ coastal survey (USCGS, 1870) confirms a persistent and natural coastal wetland setting. The age of unit **Qm** is constrained to less than about 6,000 yr BP because before that time, sea level was too low to deposit beach sediment at or above present-day sea level (Eronen and others, 1987; Dragovich and others, 1994; Mosher and Hewitt, 2004).

#### LATEST PLEISTOCENE TO HOLOCENE NONGLACIAL DEPOSITS

- Qp Peat**—Organic and organic-rich sediment; includes peat, gyttja, muck, silt, and clay; typically in closed depressions; 10 ft thick along peat survey line Rigg A (secs. 23 and 24, T29N R1W), 24 ft thick along peat survey line Rigg D (sec. 34, T29N R1W), and 44 ft thick along Rigg C (secs. 22 and 23, T29N R1W) (Rigg, 1958); unit thickness unconstrained elsewhere; mapped in wetland areas and flat-bottomed closed depressions unless a different unit was identified; commonly identified based on prior thematic mapping (Rigg, 1958; USDA, 2009), consideration of topography, and (or) infrared and color aerial photos.
- Qls Landslide deposits**—Cobbles, pebbles, sand, silt, clay, boulders, and diamicton in varied amounts within landslide bodies and toes; clasts and grains angular to rounded; unsorted; generally loose, jumbled, and unstratified, but locally retains primary bedding and compaction; commonly includes liquefaction features. Absence of a mapped slide does not imply absence of sliding or hazard. Many slide areas are unmapped because they are too small to show at map scale, or because steep slopes, beach waves, or streams have dispersed their deposits. Slides not recognized with confidence are shown as unit **Qmw**. Some slide areas include exposures of underlying units.
- Qmw Mass-wasting deposits**—Cobbles, pebbles, sand, silt, clay, boulders, or diamicton, in varied amounts; typically loose; generally unsorted; locally stratified; mapped along mostly colluvium-covered or densely vegetated slopes that are potentially or demonstrably unstable; locally includes alluvial fans, debris fans, landslides too small to show separately or those that could not be confidently mapped, and exposures of underlying units. Absence of a mapped mass-wasting deposit does not imply absence of slope instability or hazard.
- Qa, Qoa Alluvium**—Sand, silt, clay, peat, pebbles, and cobbles along some active or abandoned channels; clasts and matrix generally gray and fresh, but some exposures iron-stained; loose; clasts typically well rounded and moderately to well sorted; stratified to massively bedded; derived from local sources and deposited in streams and on flood plains. Unit **Qa** resembles and likely includes relict alluvium (units **Qoa** and **Qgo**) and was mapped where we were unable to infer a lack of geomorphic activity in the modern environment. Unit **Qoa** likely includes many recessional glacial deposits.

**Qaf, Qoaf** **Alluvial fan deposits**—Pebbles, sand, cobbles, boulders, and silt, in varied amounts; gray to brown; loose; moderately to poorly sorted; stratified to poorly stratified; derived from local sources and deposited in concentric lobes where streams emerge from confining valleys. Deposition is commonly sudden, hazardous, and associated with significant storm events. We mapped unit **Qoaf** where we inferred a lack of geomorphic activity in the modern environment. Relict fan deposits (unit **Qoaf**) have stopped accumulating because modern valleys lack active channels or because streams are sufficiently incised to preempt addition of modern sediment.

## PLEISTOCENE GLACIAL AND NONGLACIAL DEPOSITS

### Vashon Drift of the Fraser Glaciation

This mapping produced seven new age analyses from advance outwash at four sites mapped as unit **Qga** (and its subunits) within the map area (Tables A1, A2, and A3). These and additional age control data that constrain the timing of events and ages of deposits from the Fraser Glaciation are discussed below in *Ages of Quaternary Units*.

**Qgo** **Vashon recessional outwash**—Sand, pebble and cobble gravel, and some silt and clay; clasts and matrix mostly fresh and gray, but commonly iron-stained to brown, red, and yellow, and in some exposures distinguished from otherwise similar, more recent alluvium (units **Qa**, **Qoa**) by more advanced weathering of unit **Qgo**; loose; clasts subrounded to well rounded; moderately sorted and stratified. We infer unit **Qgo** to be widespread in the subsurface beneath peat bogs and alluvial valley bottoms, with pebbly to cobbly facies of northern-sourced clasts inferred beneath unit **Qp** in the Chimacum Valley at the northeast map corner. Unit was deposited in a setting with a high sedimentation rate by glacial meltwater. See *Glacial Lakes, Shorelines, and Everson Interstade Marine Incursion* for discussion of recessional lake and delta deposits. Subdivided into:

**Qgos** **Vashon recessional outwash sand**—Sand and some beds and lenses of pebbles, silt, and clay; gray to pale brown; clasts moderately to well rounded; moderately to well sorted and stratified; loose and generally less compact than glacially overridden outwash sand (units **Qgas** and **Qpos**); deposited by overland flow or as slackwater deposits into a recessional lake or marine water. Surface elevations between 115 ft and 130 ft in parts of the West and Chimacum valleys (secs. 13, 14, 15, 22, 23, and 26, T29N R1W) suggest that deposition there may have been partly marine because the valley floor is below the elevation of the glaciomarine delta-front slope break at Adelma Beach (4 mi north of the map area, Schasse and Slaughter, 2005).

**Qgof** **Vashon recessional glacial lake deposits**—Silt, sand, clay, and rare dropstones; gray; loose, locally moderately indurated; moderately to well sorted; laminated or massive; inferred to be slackwater deposits in recessional lakes.

**Qgod** **Vashon recessional glacial delta deposits**—Sand with silt and lenses of gravel; gray to pale brown; loose; moderately sorted; moderately indurated and cohesive; porous to locally nonporous. Composition and character resemble unit **Qgom<sub>d</sub>** of Schasse and Slaughter (2005) 1 mi north of the map area (secs. 8 and 17, T29N R1W). At Fairmont (0.7 mi southeast of northwest map corner), well records suggest a unit thickness of at least 74 ft, but field notes in conjunction with topographic analysis of slope morphology suggest more than 100 ft. The unit was deposited by meltwater and is tentatively inferred to be marine-deltaic at Fairmont, but freshwater near the southwest map corner, where we infer it was deposited at the shore of an ice-dammed lake, possibly Lake Russell.

**Qgic** **Vashon ice-contact deposits**—Diamicton (ablation till, flow till, and lodgment till that is poorly compacted or spatially limited), pebble and cobble gravel, sand, lacustrine mud, and isolated boulders; pale- to ash-gray, ranging to tan or brown; in places lightly weathered; loose to compact; in most exposures more porous than unit **Qgt**; poorly to well sorted; massive to well stratified; locally includes over-steepened beds that developed (1) due to sub-ice flow dynamics, (2) as collapse features following melting of nearby ice, or (3) by glacio?-tectonic deformation. Unit thickness ranges from a few feet to

more than 100 ft. Unit Qgic was deposited by meltwater and ice, mostly late in the Fraser Glaciation. The unit typically coincides with landforms associated with stagnant ice, such as topographic ripples on flutes, disrupted surfaces on and between flutes, kettles, hummocky topography, and subglacial or subaerial outwash channels. Where morphologic evidence for stagnant ice is weak or absent, unit Qgic is mapped where till matrix is absent or contains less mud than is commonly found in the matrix of well developed lodgment till (unit Qgt), and the deposit is more friable than well developed lodgment till. Where stagnant-ice features are found (and mapped as unit Qgic), lodgment till is commonly absent or only a few feet thick, locally ranges to “sub-glacially reworked till” (Laprade, 2003, p. 216), and tends to be more permeable and less compact than well developed lodgment till. Much of the unit thus forms no aquitard; elsewhere, the aquitard is more “leaky” (Polenz and others, 2010, p. 13) than is typical in unit Qgt. For additional discussion of the Fraser Glaciation, leaky aquitards associated with till, and similarities among units Qgo (and subunits Qgos, Qgof, and Qgol) and Qgic east and south of the map area, see also Haugerud (2009), Polenz and others (2009a,b, 2010, 2011), and Contreras and others (2012a,b,c).

**Qgt Vashon lodgment till**—Diamicton (mostly lodgment till, typically capped by 1–5 ft of ablation till) consisting of clay, silt, sand, pebbles, and cobbles, in varied amounts, and isolated boulders typically supported by a hard, muddy to sandy matrix; gray to brown, ranging to tan; usually lightly weathered or unweathered; compact, and where well developed, resembling concrete (commonly referred to as ‘hardpan’), but commonly hackly or looser near the surface, with loose ablation till comprising the upper 1 to 10 ft; in most exposures less porous than unit Qgic; clasts occasionally striated and faceted with subangular or rounded edges; unsorted; unstratified (but locally banded); forms a patchy cover, with typical exposures 3 to 15 ft thick. Unit Qgt was deposited directly by glacial ice. Plutonic, basaltic, and metamorphic erratic boulders are common in and on till. Some exposures include locally sheared and jointed lenses or layers of sand, pebbles, and cobbles. Unit Qgt covers many fluted surfaces but is commonly discontinuous. Well developed lodgment till locally forms an effective aquitard, but varied till thickness and association (in some instances gradational) with more permeable ice-contact deposits and outwash channels suggest that the aquitard is leaky at map scale (Haugerud, 2009; Polenz and others, 2009a, 2010; Contreras and others, 2012a,b,c).

We mapped unit Qgt where we observed stronger lodgment till development—and typically also better development of fluting—than where we mapped unit Qgic. We include in unit Qgic other ice-contact deposits and typically observed less lodgment till development than in unit Qgt. We typically associate unit Qgic with stagnant ice near the end of the glaciation, but were motivated by well records to locally show unit Qgt upsection of unit Qgic. Unit Qgt is typically in sharp, unconformable contact with underlying units. Unit Qgt lies stratigraphically below unit Qgo and above unit Qga.

**Qga Vashon advance outwash**—Sand, and less commonly pebble or (and) cobble gravel, silt, or (and) clay; gray to tan; generally compact (see fig. 4 of Polenz and others, 2009a), but commonly cohesionless; clasts typically well rounded and well sorted; mud content low in sandy or pebbly facies, except in ice-proximal deposits and isolated instances in glaciolacustrine deposits that include diamicton from debris flows or floating ice; very thinly to very thickly bedded, with planar beds forming the dominant facies in widespread lacustrine deposits; also includes graded beds, cut-and-fill structures, trough-and-ripple crossbeds, and foresets, but ranges to structureless. Sand mineralogy is dominantly monocrystalline quartz (30–50%), polycrystalline quartz (10–15%), plagioclase feldspar (1–2%), and potassium feldspar (1–2%), with lesser opaques and lithics.

Unit Qga was deposited as proglacial, fluvial, deltaic, and lacustrine outwash during the Vashon glacial advance and is northern sourced. Well record W35 and field observations of subunits Qgaf and Qgas suggest that unit thickness may reach about 380 ft near the northeast map corner (sec. 23, T29N R1W). This unit (Qga) is typically overlain by units Qgt or Qgic along a sharp, unconformable contact. We use seven new age analyses from advance outwash at four sites within the map area (Tables A1, A2, and A3), and several age estimates from outside the map area, to place the age of unit Qga between 20 and 17.5 ka (see *Ages of Quaternary Units*). However, we note that age-control data for Vashon-age ice arrival at the map area and similar latitudes in the Puget Lowland appear paradoxically old compared

to age-control data from the southern Puget Lowland. The unit may include some unrecognized older deposits (see also unit Qc<sub>o</sub>). Subdivided into:

- Qgas** **Vashon advance outwash sand**—Sand, in some exposures pebbly or with interbeds of silt, clay, pebbles, cobbles, or diamicton; pale gray to tan; generally compact; particles typically subrounded or well rounded and moderately to well sorted; locally massive, but more commonly very thinly to very thickly bedded. Planar (generally lacustrine) beds comprise most of the unit in the map area, but the unit also contains graded (mostly fluvial) beds, cut-and-fill structures, trough-and-ripple crossbeds, and foresets. Field observations suggest 220 to 300 ft unit thickness near the northeast map corner (sec. 23, T29N R1W).
- Qgaf** **Vashon advance lacustrine mud**—Glaciolacustrine silt, ranging to clay, locally with dropstones or interbeds of sand, pebbles, cobbles, or diamicton; gray to tan; compact; moderately to well sorted; planar-laminated to massive. Well record W35 and field observations suggest that unit thickness may reach 180 to 200 ft near the northeast map corner (sec. 23, T29N R1W).

### Sediments Older than the Vashon Stade

- Qc** **Pre-Vashon nonglacial deposits (cross section only)**—Sand, and less commonly clay or clayey sand, in places containing wood; mostly gray, less commonly brown; compact. We based mapping of unit Qc on well logs that noted wood amid sand or clay, and thus have no data on sedimentary structure and mineralogy. The age of unit Qc may span multiple nonglacial periods. Where identified from well records, the unit is interpreted as nonglacial based on the presence of wood, which we assume to be more likely in a nonglacial setting than in a glacial setting. Subdivided into:
- Qc<sub>o</sub>?** **Olympia nonglacial deposits**—Sand, and less commonly silt, pebble gravel, minor clay, and minor peat; mostly gray to tan, locally brown or bluish gray; compact; moderately sorted; mostly horizontally planar-bedded, for which we suggest a lacustrine setting; some low-angle crossbeds. Most grains are subangular to subrounded. We observed 25% quartz, 10% polycrystalline quartz, 3% potassium feldspar, >1% amphibole, 1% plagioclase, 1% opaque minerals, minor micas and mafic minerals, and 5–7% unidentified grains. Minor microveins can be seen in polycrystalline quartz and suggest that at least some northern-sourced grains are present (Polenz and others, 2012c). Unit Qc<sub>o</sub>? is mapped where an Olympia nonglacial age is tentatively inferred in deposits exposed along drainages on the southern map boundary (secs. 33–34, T28N R1W), but we note that our constraints on age and depositional environment equally support mapping these deposits as Vashon advance outwash (see also *Ages of Quaternary Units*).
- Qpu** **Undivided Quaternary sediment older than Vashon Till**—Sand, pebble gravel, silt, clay, diamicton, organic sediment, and boulders, in varied amounts; color and weathering varied; compact; varied grain size, rounding, sorting, and bedding. Shown where sediment age, paleoenvironmental association, and sources were unconstrained or enigmatic (see also *Ages of Quaternary Units*). Although generally mapped as pre-Vashon, the unit may include Vashon advance outwash.

### Tertiary Sedimentary and Volcanic Bedrock

Most bedrock units in the map area are Eocene in age. For Eocene sedimentary rock units above a mid-Eocene regional unconformity, Walsh and others (1987) and Dragovich and others (2002) included a subscript 2 in the unit symbol; for rocks below the same unconformity, a subscript 1; absence of a subscript numeral indicated absence of constraint to either above or below the unconformity. We continue this convention.

- ØEm** **Undifferentiated sedimentary rocks (late Eocene to early Oligocene)**—Marine mudstone, siltstone, and less commonly sandstone and claystone; medium to dark gray, but in most exposures lightly to moderately weathered pale to dark brown, reddish brown, yellowish brown, and tan; grains angular to subrounded; moderately to well sorted; bedding planar and commonly faint; commonly hackly and

(or) marked by spheroidal weathering. Some exposures are barely recognizable as bedrock and are fragile or weathered enough to be crushed between fingers. Petrographic examination revealed quartz (10–40%, including 1–3% polycrystalline quartz; one sample at age site GD15, sec. 20, T28N R1W, contained 15–20% polycrystalline quartz), potassium feldspar (3–10%), plagioclase (1–7%), muscovite (0–10%), and opaque minerals (3–10%, but 20% at age site GD15). Some samples are calcareous, at least in part due to secondary calcite cement. Fine-grained samples are 40 to 80 percent clay matrix. Slight metamorphism to slate or phyllite is suggested by sericitic and (or) chloritic alteration and slight alignment of mineral grains in some samples, such as at age sites GD14, 15, and 20 (secs. 17, 20, and 29, T28N R1W, respectively) and age sites GD17 and 22 (sec. 9, T28N R1W). Unit  $\Phi$ Em was mapped where exposures did not clearly or exclusively align with known characteristics of other sedimentary rock units. We identified the unit near exposures of the sandstone of Snow Creek along the south half of the western map edge and near exposures of Townsend Shale in the south-central part of the map area; we did not map these units in those areas because we were unconvinced that our observed exposures sufficiently resembled known occurrences of those units, but, for similar reasons, we did not assign them to other specific units. We also mapped unit  $\Phi$ Em along the east side of West Valley 1.3 to 2.5 mi south of the northern map edge. In light of the absence of stratigraphic or radiometric age-control data, the unit is classified as Oligocene to Eocene because the geographic distribution and sandstone to claystone textures suggest association with units Em<sub>2ss</sub>, Em<sub>2t</sub>, and (or) upsection units such as the Oligocene–Eocene Quimper Sandstone or Marrowstone Shale (not mapped).

**Em<sub>2t</sub> Townsend Shale (late Eocene)**—Marine mudstone, siltstone, and sandstone; commonly micaceous; some exposures contain secondary calcite; gray where fresh, brown, dark gray, or pale olive-brown to reddish brown in weathered exposures; commonly weathers spheroidally to form hackly debris in outcrop; mudstone dominantly clay-rich matrix (70–80%), with 20 to 30 percent fine sand composed mainly of quartz, polycrystalline quartz, plagioclase, and potassium feldspar; bedding is undulatory. Tabor and Cady (1978) noted overturned bedding at age site GD11 (sec. 17, T28N R1W); we were unable to confirm or deny this observation but sampled mudstone from the base of a roadside ditch at this site. The above description is based mainly on exposure at age site GD5, 0.4 mi north of the southern map boundary (sec. 33, T28N R1W), where Spencer (1984) mapped Townsend Shale. We sampled the unit at age sites GD5, GD11, GD10 (sec. 32, T28N R1W), and GD19 (sec. 28, T28N R1W) and did not identify it elsewhere. Our samples from age site GD19 are calcareous and effervesce on HCl tests. A mudstone thin section from age site GD5 resembles that from GD11, where E. Nesbitt (written commun., 2014) noted entirely pyrite-replaced foraminiferal casts, consistent with both Durham's (1944) characterization of the unit as pyritic and Spencer's (1984) mention of pyrite replacements of foraminiferal tests in Townsend Shale (and no other unit). Our petrographic review of unit Em<sub>2t</sub> produced no evidence of metamorphism towards slate or phyllite, but our samples of unit Em<sub>2t</sub> were so fine-grained that we could have missed the mineral grain alignment and alteration to sericite and chlorite that we used as evidence of metamorphism in unit  $\Phi$ Em. We mapped unit Em<sub>2t</sub> as late Eocene based on prior age assignment by Durham (1944), McMichael (1946), Allison (1959). Spencer (1984) further supported this age assignment by documenting upper Narizian foraminifera in the unit near the map area.

**Em<sub>2ss</sub> Sandstone of Snow Creek (late Eocene)**—Marine sandstone, siltstone, and mudstone; gray to pale grayish tan to medium brown, weathers tan; shallow exposures are weathered; coarser sediments are mostly well to moderately sorted, angular to subangular, and equigranular; finer matrix material is either clay or calcareous cement (as previously noted by Spencer [1983, 1984] along the 'Donovan Creek section' 2.9 mi south of the map area, sec. 13, T27N R1W). Bedding is thin, ranging from planar to undulatory. Petrographic examination revealed dominantly quartz (30–60%), with lesser potassium feldspar (3–10%), muscovite (3–7%), polycrystalline quartz (0–2%), and few to no mafic minerals and plagioclase feldspar. Microcrystalline polycrystalline quartz (chert) is less common than in the Lyre Formation sandstone (unit Em<sub>2ls</sub>) in the northwest portion of the quadrangle. The sandstone of Snow Creek is well exposed along Center Road (formerly Griffith Road) 2.5 mi south of the map area (age site GD8 of Contreras and others, 2014, sec. 13, T28N R1W). Samples from the Center quadrangle have yielded some foraminifera, but no biostratigraphically restrictive records. However, exposures of the unit along Snow Creek (0.9–2.3 mi west of the map area, secs. 9–11, T28N R2W [Spencer, 1984; Haussler

and others, 1999; Tabor and others, 2011]) have yielded fossils, including foraminifera that Spencer interpreted as characteristic of the upper Narizian *Amphimorphina jenkinsi* zone of the upper Eocene. Constraints on age are further discussed below (*Bedrock Stratigraphy and Paleontology*).

#### LYRE FORMATION (MIDDLE EOCENE)

**Em<sub>21s</sub> Lyre Formation sandstone and mudstone**—Marine sedimentary sandstone, fine-grained to granule, and minor thin-bedded, interbedded siltstone; overlies and is interbedded with conglomerate (unit Em<sub>21c</sub>). Sandstone is lithic- and quartz-rich, light olive gray, thick bedded, and well indurated. Most clasts are chert. Also present are clasts of mudstone, quartzite and other high-grade metamorphic rocks, quartz, and basalt. We did not observe the upper or lower contact of the unit. We identified Lyre Formation sedimentary rocks in the northwest quarter of the map area. Despite interbedding of sandstone and conglomerate, we observed the sandstone consistently southeast of the conglomerate facies and infer that the sandstone is generally upsection. Unit Em<sub>21s</sub> may therefore be the same age as the late-Eocene sandstone of Snow Creek, which we mapped as separate unit based on mineralogic distinctions (see also *Bedrock Unit Stratigraphy and Paleontology*). We mapped Lyre Formation conglomerate and sandstone in contact with the radiometrically dated middle-Eocene volcanic unit Evt<sub>1</sub> and infer that Lyre Formation sedimentary rocks bracket or interfinger with unit Evt<sub>1</sub>. Lyre Formation sedimentary rocks that contain foraminifera are assigned to the upper Narizian Stage (Snively, 1983). Constraints on unit age are further discussed below and by Weaver (1937), Brown and others (1956), Snively (1983), Spencer (1984), and Rau (2004).

**Evt<sub>1</sub> Lyre Formation volcanic tuff and breccia**—Hornblende dacite to andesite breccia with rare interbeds of lithic tuff; previously described (mostly or entirely based on exposures outside the map area) as dacitic and andesitic (Tabor and Cady, 1978; Gower, 1980; Schasse and Slaughter, 2005; Tabor and others, 2011); typically light to medium gray, pale red, and pale reddish gray; weathers brown, tan, and pale gray. Petrographic analysis revealed that breccia clasts (autoliths) are more altered than the breccia matrix. Some breccia beds are more than 40 ft thick, massive, and moderately to poorly sorted. The breccia matrix is finer grained than the autoliths and resembles interbedded tuff. Autoliths range from pebbles to boulders, are subrounded to subangular, and porphyritic with phenocrysts of euhedral and broken zoned plagioclase, hornblende, quartz, and opaque oxides and scarce glomerocrysts of hornblende and plagioclase. Tuff interbeds are rare—we observed only a single, 1-ft-thick, crystal-rich tuff in the map area (geochemistry sample G6, sec. 21, T29N R1W). The interbed is fine grained with coarse, sand-sized autoliths of older pyroclastic deposits. Petrography revealed the interbed to be porphyritic and microporphyritic with phenocrysts of plagioclase, hornblende, quartz, and opaque oxides in a finely crystalline groundmass rich in plagioclase. Chloritic alteration in angular inclusions of glass is readily observed in thin sections of the tuff interbed. Based on geochemical traits (Table M2 on map sheet), we agree with Hahn and others (2004) and Tepper and others (2004) that the unit is an adakite. The fact that clasts are more altered than the surrounding matrix implies that alteration occurred prior to eruption (Jeff Tepper, Univ. of Puget Sound, oral commun., 2014; Daniel Eungard, Wash. Div. of Geology and Earth Resources, oral commun., 2014). Tepper added that embayed and (or) rounded margins of some crystals within the tuff suggest magmatic resorption. Hahn and others (2004) estimated that the exposed section at Anderson Lake (1 mi north of the Center quadrangle) is 300 ft thick. They suggested it was deposited within topographic constraints, such as a paleovalley, and that it is unlikely to have traveled more than 6 mi from its source—consistent with a high crystal content we observed in all samples. Hahn and others (2004) and Tepper and others (2004) noted similarity to slightly older adakites in the Bremerton Hills about 22 mi south of the map area, and Wolfe and Tepper (2004) reported adakites at Mt. Zion (Fig. M1). Wolfe and Tepper (2004) also noted slight chemical differences among adakites from the various localities. New geochemical analyses (Table M2) reveal dacite, andesite, trachydacite, and trachyandesite, consistent with the analyses of Schasse and Slaughter (2005)(Fig. M2). Unit thickness appears to exceed 260 ft north of Gibbs Lake (secs. 21 and 28, T29N R1W). Schasse and Slaughter (2005) used a  $46.62 \pm 0.56$  Ma  $^{40}\text{Ar}/^{39}\text{Ar}$  date from 1.5 mi north of the map area (sec. 10, T29N R1W) to confirm the middle Eocene age of this unit.

- Em<sub>2</sub>c Lyre Formation conglomerate**—Marine sedimentary conglomerate with lenses of fine-grained to granule sandstone; underlies and is interbedded with sandstone (unit Em<sub>2</sub>s) and minor thin-bedded siltstone. The conglomerate facies includes lenses and channel bed deposits of well indurated, well rounded, thin- to very thick bedded pebble to cobble conglomerate and pebbly sandstone. Conglomerate clasts are gray to black and mostly chert. Clasts of mudstone, quartzite and other high-grade metamorphic rocks, quartz, and basalt are also present. Sandstone interbeds are lithic and quartzose, light olive gray, thickly bedded, and well indurated. Unit thickness exceeds 200 ft in a continuous section east of City Lake (sec. 20, T29N R1W); we did not observe the upper or lower contact. We identified Lyre Formation sedimentary rocks in the northwest quarter of the map area. We identified no Aldwell Formation (stratigraphically below the Lyre Formation) within the map area, and we infer an unconformable contact with underlying Crescent Formation. Despite interbedding of the sandstone and conglomerate facies, we observed the sandstone facies consistently southeast of the conglomerate and infer that the conglomerate is generally downsection of the sandstone facies and the radiometrically dated middle-Eocene volcanic unit Evt<sub>1</sub> (see also unit Em<sub>2</sub>s). Constraints on unit age are further discussed below (*Bedrock Stratigraphy and Paleontology*) and by Weaver (1937), Brown and others (1956), Snively (1983), Spencer (1984), and Rau (2004). Unit Em<sub>2</sub>c includes conglomerate that Gower (1980) and Yount and Gower (1991) mapped separately as unit Tc (described in Yount and Gower [1991] as “Unnamed Conglomerate East of Port Discovery”). Gower (1980) and Yount and Gower (1991) asserted that an angular unconformity separates steeply east-dipping Lyre Formation conglomerate from their gently east-dipping unit Tc. A regional upward-fining trend among the Eocene to Oligocene marine sedimentary rocks within the northern Olympic Peninsula suggests that unit Tc of Gower (1980) and Yount and Gower (1991) is stratigraphically below the sandstone facies of the Lyre Formation (unit Em<sub>2</sub>s). We refer to this regional trend and lithologic and textural similarity of these two chert-dominated conglomerate units (Lyre conglomerate and unit Tc) as indication that they are best mapped within the same unit.
- Em<sub>1</sub>c Crescent Formation sedimentary rocks**—Volcaniclastic basaltic pebble, cobble, and boulder conglomerate and locally calcareous sandstone and mudstone; dark gray, reddish dark brown, and black; matrix commonly weathered to rotten, muddy–clayey sand; modal particle size varies with exposures and ranges from mud grains to boulders; subangular to subrounded; poorly sorted. Unit thickness is poorly constrained—well record W14 (sec. 25, T29N R2W) suggests a thickness of 37 ft near the western map edge, but we caution that we did not field-locate this well and were unable to verify the accuracy of its location. West of the map area, Spencer (1984) observed 232 m (760 ft) of section and that the contact with underlying basalt (unit Ev<sub>c</sub>) is irregular, undulatory, and directly overlain by limestone pods and breccia. Spencer (1984) used fossils from within Crescent Formation sedimentary rocks to argue that these deposits are sourced from Crescent Formation basalt. In the Center quadrangle, calcareous mudstone samples from age site GD16 contain macrofossils, but during preliminary analysis these samples yielded no age constraints (Nesbitt, written and oral commun., 2014). Constraints on unit age are further discussed below (see *Bedrock Stratigraphy and Paleontology*) and by Arnold (1906), Brown and others (1960), Rau (1964, 1981, 2000, 2004), Cady and others (1972a,b), Wolfe and McKee (1972), Whetten and others (1988), Squires and others (1992), Hirsch and Babcock (2009), and Polenz and others (2012a,b,c).
- Ev<sub>c</sub> Crescent Formation basalt**—Basalt in massive flows, as breccia, and rare pillows; medium to pale gray and dark gray where fresh, weathers gray and medium yellowish brown; commonly displays spheroidal exfoliation. Petrographic examination reveals dominantly cryptocrystalline basalt groundmass with disseminated opaque minerals. Some thin sections have broken plagioclase and a few samples include localized zones of oxidation, calcite mineralization, and quartz veining. Aphanitic flows commonly include amygdules of zeolite and chalcedony, and phenocrysts of plagioclase, olivine, and—separately or in glomeroporphyritic rafts—augite and hypersthene. Whole-rock analysis of one basalt sample reveals chemical attributes typical of Crescent Formation basalt (Fig. M2) and island-arc tholeiite (Table M2), consistent with the upper Crescent Formation (Glassley, 1974; Babcock and others, 1992). Our mapping of Crescent Formation basalt near the northwest map corner generally confirms but differs in detail from prior mapping of the distribution of Crescent Formation basalt (Tabor and Cady, 1978; Gower, 1980;

Yount and Gower, 1991) or of unnamed basaltic volcanic rock (Spencer, 1984; Grimstad and Carson, 1981). No Crescent Formation samples from the map area have been dated, but several studies support early to middle Eocene age. Constraints on unit age are further discussed below (*Bedrock Stratigraphy and Paleontology*) and by Arnold (1906), Allison (1959), Brown and others (1960), Rau (1964, 1981, 2000, 2004), Cady and others (1972a,b), Wolfe and McKee (1972), Spencer (1984), Whetten and others (1988), Babcock and others (1992, 1994); Squires and others (1992), Hirsch and Babcock (2009), and Polenz and others (2012a,b,c).

## RESULTS, FINDINGS, AND OBSERVATIONS

### Bedrock Stratigraphy and Paleontology

Like Weaver (1937), Allison (1959), and Spencer (1984), we see a systematic distribution of bedrock in the map area, from oldest units in the northwest to progressively younger units in the southeast, which at map scale suggests an overall southeast dip of bedding, despite considerable scatter among measured bedding orientations. The oldest rocks are early to middle Eocene Crescent Formation basalt (unit Ev<sub>c</sub>) and sedimentary rocks (unit Em<sub>1c</sub>) near the northwest map corner. Middle Eocene Lyre Formation (units Em<sub>2lc</sub>, Em<sub>2ls</sub>, Evt<sub>l</sub>) is exposed southeast of (and stratigraphically above) the Crescent Formation. Contacts between the two formations are unconformable and typically coincide with northeast- and east-trending inferred faults. Late Eocene sandstone of Snow Creek (unit Em<sub>2ss</sub>) is exposed south of the Lyre Formation in the western half of the quadrangle and may be stratigraphically equivalent to sandstone within the upper Lyre Formation (unit Em<sub>2ls</sub>). Younger Eocene Townsend Shale (unit Em<sub>2t</sub>) and Eocene to perhaps Oligocene sandstone and mudstone (unit ØEm) are exposed east of the sandstone of Snow Creek. However, the pattern of younger bedrock to the southeast is reversed just outside the map area: younger (Oligocene–Eocene) rocks are exposed within 1.5 mi north of the quadrangle (Allison, 1959; Spencer, 1984; Rau, 2004; Schasse and Slaughter, 2005), older Crescent Formation basalt 0.8 to 4.3 mi east of the south half of the quadrangle (sec. 3, T27N R1E; Grimstad and Carson, 1981; Yount and Gower, 1991; Contreras and others, 2013), and Aldwell and Crescent Formations about 5.5 mi south of the southwest map corner (Tabor and Cady, 1978; Spencer, 1984; Yount and Gower, 1991; Contreras and others, 2014).

Ages and character of bedrock units in the Center quadrangle are almost entirely defined on the basis of data from outside the quadrangle. Howard Gower collected two fossil samples with foraminifera from the Center quadrangle (Rau, 2004, records 3245 and 3246, both from “250 m E, 600 m S, NW cor. sec. 29, T29N R1W”—age site GD23). Rau characterized the foraminiferal assemblages from both samples as Narizian, consistent with our mapping of Lyre Formation sandstone (unit Em<sub>2ls</sub>). Rau (2004) also reported 38 Eocene and Oligocene samples from surrounding 7.5-minute quadrangles. Pat Spencer (1984) reported many additional fossil samples from the Uncas quadrangle west of Center and fewer from the Quilcene quadrangle south of Center. He reported none from the Center quadrangle but commented (written commun., 2014) that he chose not to report sample sites that yielded no fossils; he identified specific bedrock units and locally reported bedding orientations in parts of the Center quadrangle. Allison (1959) similarly mapped bedrock units, showed some field stations and bedding orientation sites, but he reported fossils only from outside the Center quadrangle.

We selected samples from 18 sedimentary bedrock sites for fossil analysis (age sites GD5–GD22) and analyses were performed by E. Nesbitt (written and oral commun., 2014). None of the samples yielded biostratigraphic constraints, at least in part because of remineralization: samples from six age sites contained quartz-recrystallized foraminiferal molds (GD5–GD10) and one sample contained entirely pyritized foraminifera (GD11). Samples from eleven sites yielded no foraminifera (GD12–GD22). A sample from age site GD22 (sec. 9, T28N R1W) may contain trace fossils. A sample from age site GD16 (sec. 30, T29N R1W) contains unidentified macrofossils that await further analysis at the Burke Museum of Natural History and Culture.

The paucity of biostratigraphic information from the map area appears to be a systematic result of the depositional history and secondary alteration of bedrock within the quadrangle, and it sets this quadrangle apart from areas to the south, east, and north. Consequently, our stratigraphic separation of units is based on texture, lithology, and field relations.

### Ages of Quaternary Units

Pre-Vashon deposits have been mapped in adjacent quadrangles (Gayer, 1976; Hanson, 1976; Schasse and Slaughter, 2005; Tabor and others, 2011; Contreras and others, 2014). Some prior mappers also interpreted some

sediments below Vashon Till in the eastern half of the Center quadrangle as pre-Vashon (Gayer, 1976; Hanson, 1976; Grimstad and Carson, 1976). However, on the basis of our field characterizations, petrographic analyses, and new age control data, we reassign most of these deposits to Vashon advance outwash (units **Qga**, **Qgas**, and **Qgaf**). Well records suggest a considerable thickness of subsurface sediment that pre-dates Vashon Till but does not necessarily pre-date Vashon advance outwash; however, because most well and boring-log descriptions are vague and insufficient for determination of specific units, we were unable to link those descriptions to surface exposures. We therefore show most of these deposits as undivided unit **Qpu**. Our mapping of unit **Qpu** at the northeastern map corner is based on prior mapping (Gayer, 1976; Grimstad and Carson, 1981; Schasse and Slaughter, 2005).

We also mapped unit **Qpu** in a drainage along the western map boundary (north and southwest of well site W14, sec. 25, T29N R2W) because sand beneath Vashon Till revealed a higher lithic fragment content (>20% among medium sand grains, ≤50% among coarse sand grains) than we observed elsewhere in the map area. This is atypical of the generally more quartzo-feldspathic sand of northern provenance that we associated with drift elsewhere in the map area. It thereby suggests an Olympic Mountains sediment-source component that favors a nonglacial setting, because it would be difficult to reconcile with Cordilleran ice in or near the map area. However, the sand could be Cordilleran-glacial advance outwash, because shallow bedrock (basalt and basaltic-lithic sedimentary rock) abounds in this part of the map area and may have provided a source for enriching otherwise distal-northern-sourced outwash sand with basaltic lithic fragments. Separately, we noted a surficial till exposure along 200 ft of roadcut mid-slope in the northern valley wall, 70 ft below the fluted upland surface and 500 ft north of well site W14 (sec. 25, T29N R2W). A distinct and sharp slope-break separates this valley wall from the fluted upland surface and suggests that the valley is post-glacially incised and therefore should not be draped with Vashon Till. A till thickness of 70 ft has been observed elsewhere in the map area, and thicker till sections are suggested by well records (Cross Section A), but the till along the midslope road could also be pre-Vashon.

We also note possible pre-Vashon till and underlying lacustrine outwash along the eastern flank of West Valley in the northeast part of the map area (significant sites S5, sec. 26, T29N R1W, and S6, sec. 23, T29N R1W), where we mapped units **Qgic** (site S5) and **Qgaf** (site S6), but prior maps (Gayer, 1976; Hanson, 1976; Grimstad and Carson, 1981) and unpublished field notes (Robert Carson, Whitman College, written commun., 2013; Kathryn Hanson, AMEC, oral and written commun., 2013) show Possession till. Well record W35 (near site S6) could be reasonably interpreted to include pre-Vashon till at a comparable elevation. If correctly identified, this pre-Vashon till may be continuous in the subsurface at slightly above 200 ft elevation between sites S5 and S6. We did not map pre-Vashon drift here because our own observations provided no indication of pre-Vashon deposits, and new luminescence age-control data we obtained upsection at the nearby age site GD2 (sec. 23, T29N R1W) corroborated our interpretation that deposits previously mapped as older are Vashon advance outwash.

We equate the nonglacial unit **Qc<sub>o</sub>** to MIS 3 (Morrison, 1991; Troost and Booth, 2008) and mapped it in some drainages along the southern map boundary (secs. 33 and 34, T28N R1W) because the drainages expose thick packages of moderately to well sorted sand (with rare pebbly lenses or interbeds) that resembles sand Contreras and others (2014) interpreted as Olympia nonglacial deposits south of the Center quadrangle. Their interpretation is supported by their luminescence dates from age sites GD6 and 7 (sec. 17, T27N R1W), 2.8 mi south of the Center quadrangle, and GD18 and 19 (sec. 3, T26N R1W), 6.7 mi south of the Center quadrangle. We queried all instances of unit **Qc<sub>o</sub>** because: (1) the exposures lack peat or other organic debris and revealed a lower feldspar content than Contreras and others (2014) typically saw south of the Center quadrangle, and (2) because unit **Qc<sub>o</sub>** where we mapped it resembles deposits that we interpreted as Vashon advance outwash (units **Qga**, **Qgas**, and **Qgaf**) elsewhere in the Center quadrangle. The interpretations of advance outwash were based on field characterizations, petrographic analyses, and seven new age estimates at four sites in the Center quadrangle (radiocarbon at age site GD1, sec. 4, T28N R1W, luminescence at age sites GD2 [sec. 23, T29N R1W], GD3 [sec. 5, T28N R1W], and GD4, [sec. 15, T28N R1W]). We mapped undivided unit **Qc** in our cross section where well logs noted wood, peat, or other organic matter amid sand, silt, or clay.

Prior to this mapping, no Quaternary age-control data from the Center quadrangle had been published. We agree with Troost and Booth (2008) that the age of Vashon Drift generally corresponds to MIS 2 (Morrison, 1991) and present seven new age-analyses from Vashon advance outwash (units **Qga**, **Qgaf**, and **Qgas**) at four sites within the map area. We further refer to several age estimates from outside the map area to estimate the ages of Vashon Drift and stratigraphically adjoining units. We note, however, that the timing of ice advance, collapse, and the Everson interstadial incursion of elevated sea water suggested by these data are difficult to reconcile with dates from the southern Puget Lowland that suggest somewhat later ice arrival and deglaciation.

Lowest in the stratigraphic section (and in elevation) among our new age sites is a radiocarbon date (between 18.47–18.30 and 18.09–17.96 ka old; Table A1) from delicate plant matter in lacustrine silt (unit Qgaf) at age site GD1 (elev. 274 ft; sec. 4, T28N R1W). Age sites GD2 (sec. 23, T29N R1W), GD3 (sec. 5, T28N R1W), and GD4 (sec. 15, T28N R1W) each provide optically (OSL) and infrared (IRSL) stimulated luminescence age estimates (Tables A2 and A3) from sand upsection of the silt at age site GD1. Our paleo-environmental interpretations and site altitudes suggest that the sediment at GD2 (lacustrine, elev. 280 ft) is oldest, followed by that at GD3 (low-energy fluvial, elev. 355 ft). We would expect age site GD4 (elev. 456 ft) to be youngest; it marks the upper end of a sandy section just below the contact with a pebbly channel deposit that we interpret as more ice-proximal advance outwash. The lab analyst interpreted all six luminescence dates as between 19 and 12 ka (Shannon Mahan, USGS, written commun., 2014) and added that the sample from age site GD4 displayed signs of partial bleaching (incomplete pre-depositional resetting of the luminescence signal due to insufficient pre-depositional exposure to light). This would inflate our age estimate for the sample, as is common in other glacial deposits (Rhodes, 2011). Incomplete resetting would therefore explain the high IRSL age estimate for that site (Tables A2 and A3). A partial bleaching problem at GD4 is thus consistent with our impression that this site is our youngest, most ice-proximal sample site, with approaching ice limiting pre-depositional light exposure and triggering a facies shift from sand to pebble gravel.

The above age estimates are consistent with radiocarbon data that suggest Vashon advance outwash arrived 16.9 mi south-southeast of the map area sometime after 20.36 to 18.92 ka (Deeter, 1979; Polenz and others, 2013). A 17.8 to 17.5 ka radiocarbon date from 10.2 mi southwest of the map area very likely post-dates Vashon ice arrival in the map area because it dates impoundment, apparently by ice of the Puget lobe, of a lake at 1,350 ft elevation in an Olympic Mountains valley at the latitude of Brinnon (Polenz and others, 2012c). We infer that age control data from within and near the map area suggest the end of Olympia nonglacial conditions before 18 ka and Vashon advance outwash deposition between 20 and 17.5 ka. These estimates are consistent with the ice-advance timeline advocated by Porter and Swanson (1998, Fig. 4) and Booth and others (2004, Fig. 9) farther east in the Puget Lowland. If valid for the western margin of the Puget Lowland, that timeline would suggest ice arrival in the map area around 18.1 to 18.2 ka.

Dates on late-Vashon ice disintegration and on post-glacial conditions constrain the end of the Vashon Puget lobe ice incursion. About 17 mi south of the map area, Polenz and others (2013, age site GD15) obtained a  $17.130 \pm 1.08$  ka IRSL age estimate for partial Puget lobe ice disintegration. We agree with Polenz and others (2013) in disregarding an OSL date from the same site because the quartz (OSL) analysis for that site proved technically challenging, as has been common among Puget Lowland glacial sediment samples. Radiocarbon data from Carpenter Lake 11.7 mi southeast of the Center quadrangle, presented by Anundsen and others (1994) and converted to calendar years by Porter and Swanson (1998), suggest ice-free conditions sometime between 16.6 and 16.2 ka (sample QI-4067). A separate sample from the same site suggests the end of glaciomarine inundation at 31 ft (9.5 m) elevation sometime between 16.7 and 15.9 ka (sample QI-4065).

The record of emergence from glaciomarine inundation at Carpenter Lake constrains the time of ice melting in the map area. A meltwater channel extends from Chimacum Valley in the map area to a glaciomarine delta complex at Adelma Beach 4 mi north of the map area (Schasse and Slaughter, 2005; Dethier and others, 1995). The channel and the delta complex strongly suggest that during and after the maximum glaciomarine sea level, at least part of the map area was still ice-covered; ice in or near the map area was required as the source of, or pathway for, the meltwater that constructed the delta. Multiple delta-front slope breaks at Adelma Beach range in elevation from 130 ft to less than 95 ft and therefore record decreasing relative sea level in the waning stages of the Everson marine inundation. We therefore see no time difference between the Everson Interstade and ice wasting late in the Vashon Stade in the map area. We infer that the post-Everson inundation date (16.7–15.9 ka) from Carpenter Lake approximates the time of ice wasting in the map area, although patches may have persisted for millennia (Porter and Carson, 1971). We conclude that age control data from within and near the map area suggest Vashon ice incursion arrived at age site GD1 in the center of the map area after 18.5 ka, but began before 17.5 ka, and ended approximately 16.7 to 15.9 ka. We note, however, that at least the Carpenter Lake (recessional) dates and GD15 of Polenz and others (2013) are so old that they are difficult to reconcile with Vashon advance dates from the southern Puget Lowland that range between 17.8 and 15.3 ka (Walsh and others, 2003; Polenz and others, 2010, 2011, 2012a,b,c).

After draining of the glacial lakes, portions of the Puget Lowland may have experienced valley incision that was followed by marine inundation and valley-floor aggradation (Schasse and others, 2009). Aggradation continued until postglacial isostatic rebound raised the crust in the Puget Lowland and caused relative sea level to drop below

modern sea level (Dragovich and others, 1994; Mosher and Hewitt, 2004), which in turn caused some valleys to incise below modern sea level. This deeper incision is recorded in drainages where loose fill in the lower reaches of postglacial valleys extends below sea level (Polenz and others, 2013; Schasse and others, 2004). We found no indication that drainages within the map area were similarly affected—most, and perhaps all, were too small or too far removed from shore to produce a record of this base-level drop. It is also unclear if ice wasting in the map area occurred early enough for drainages to develop at that time.

The presence of a voluminous meltwater source in Chimacum Valley (and perhaps West Valley) at the time of maximum glaciomarine inundation suggests that at least some of the map area remained ice-covered until after the inundation. However, we propose that the record of vigorous early postglacial incision elsewhere in the Puget Lowland suggests that drainages in the map area were substantially incised by meltwater at the end of the Vashon Stade. Although these processes have been much less dynamic since, as elsewhere in the Puget Lowland, headward erosion, valley incision, and associated mass wasting and alluvial deposition clearly continue. The implication for sedimentary units in the map area is that most alluvial fans and valley fill likely date to the time of ice melting. Consequently, we suggest that units Qoa and Qoaf and much or most of units Qa and Qaf were deposited during ice melting, although we lack definitive indications to document this.

The above discussion suggests that post-Vashon ice-free conditions occurred sometime near 16 ka. USGS Fact Sheet 2010-3059 places the age of the Holocene–Pleistocene boundary at 11,700 ±99 yr and we therefore distinguish between Holocene units (af, Qb, Qm) and units that range from Pleistocene to Holocene age (Qp, Qls, Qmw, Qa, Qoa, Qaf, Qoaf). We limit units Qb and Qm to the late Holocene because before about 6,000 years ago, sea level was much lower (Dragovich and others, 1994; Mosher and Hewitt, 2004), and these deposits could only have formed when sea level was near its present level.

### **Glacial Lakes, Shorelines, and Everson Interstade Marine Incursion**

Ice-dammed lakes filled large parts of the Puget Lowland during deglaciation (Bretz, 1910, 1913; Thorson, 1980). Shorelines and deltas above Hood Canal document two prominent lake levels well above modern sea level (Bretz, 1910, 1913; Thorson, 1980, 1981, 1989; Waitt and Thorson, 1983; Booth and others, 2004; Polenz and others, 2012a,b,c). Hagerud (2009) recognized at least five lake levels on the Kitsap Peninsula, but it remains unclear whether any of these lakes extended into the map area. Thorson (1980) suggested that the valley north and south of Leland Lake along the western edge of the Center quadrangle contains lake sediment below 197 ft elevation and served as a north-draining lake spillway to Port Discovery. In the Center quadrangle, we did not observe lake sediments or evidence for such a lake drainage near Lake Leland. However, we interpreted the morphology of an isolated landform 1 mi north and 0.4 mi east of the southwest map corner as evidence for a delta deposit (unit Qgod) that suggests a relict shore between 459 and 483 ft elevation—consistent with the ~459 ft elevation expected of the uppermost large Vashon recessional ice-dammed lake in the Hood Canal basin. In order to recognize possible relict lake (and marine) shores elsewhere in the map area, we scrutinized lidar-based images in search of landforms that suggest relict shores (with simulated sun angles at 90 degrees and at 45 degrees to the north, northeast, east, southeast, south, southwest, west, and northwest; some renderings blended multiple sun angles and/or contours, and we excluded some candidate features based on additional review of parcel data and land use patterns evident on aerial photos). We digitized (but did not document in this report) more than 300 possible or definite shorelines. Most features are isolated landforms and very few of them unambiguously document shorelines. Based on elevation, a cluster of candidate features in the southeastern quarter of the map area could relate to the same elevated lake as unit Qgod near the southwest map corner. The slopes above West Valley, in the northeastern quarter of the map area, revealed candidate features at many elevations that suggest a record of progressive base-level lowering, but at no elevation could we definitively identify these as lake shore(s), much less as evidence of a single, large lake within the valley. We encountered extensive deposits of silt, sand, and silty sand only near the valley floor. Most of these deposits were too compact to suggest recessional glacial-lake sediment and were instead mapped as older lake deposits (units Qga, Qgas, Qgaf, Qpf).

We mapped likely recessional lake deposits as units Qgof and Qgos between 240 and 180 ft elevation in West Valley in and adjacent to sec. 9, T28N R1W, but these deposits could also be outwash flood-plain deposits. However, we also identified probable shoreline segments (not shown) at multiple elevations near these deposits, which we interpret as added evidence that the deposits are lacustrine. Among the possible shorelines in West Valley, those at about 240 and 215 ft are the most extensive and prominent. We identified few similar features or deposits at similar elevations farther north in West Valley and none farther south in Tarboo Creek valley. We infer

that the lake may have been localized. If a larger lake was present, we suspect that it extended only to the north in West Valley (and not south along Tarboo Creek).

Additional probable shorelines at about 190 and 170 ft elevation occur farther north in West Valley (secs. 3 and 4, T28N R1W, and secs. 34 and 35, T29N R1W), and we observed corresponding(?) deposits of unit Qgof between 180 and 140 ft. Farther north, we were unable to distinguish possible shorelines at similar and lower elevations from possible kame landforms and other outwash terraces. Elevation and geomorphic continuity suggest that sand of unit Qgos between 160 and 117 ft elevation in West Valley (secs. 22, 23, 27, and 28, T29N R1W) is associated with the Everson marine incursion that formed a delta-front slope break at 130 ft at Adelma Beach 4 mi north of the map area (Schasse and Slaughter, 2005; Dethier and others, 1995). This sand may therefore be partly glaciomarine. Compared to Chimacum Valley (farther east and mostly outside the map area), West Valley is sprinkled with irregular ice-contact deposits and contains gently sloping valley sides and an uneven valley width. This morphology and the northward transition from unit Qgof (mud) to unit Qgos (sand) within the Vashon recessional lacustrine sediment below 180 ft suggest that Vashon recessional meltwater did little to shape the valley. The lacustrine deposits may instead be slackwater flood deposits from meltwater that invaded the map area from Chimacum Valley northeast of the map area.

We tentatively interpret a relict delta-front slope break at Fairmont (0.7 mi southeast of northwest map corner) as Everson interstade marine shore. This delta-front slope break rises gently from 123 ft at the western map edge to 139 ft at the east end of the feature and approximates the elevation of the demonstrably marine relict shore at Adelma Beach. We do not know why the Fairmont shore elevation drops westward but caution that the delta-front slope break is not very clearly expressed, and our elevation statements are therefore only approximate.

## Structure

The Center quadrangle is in the western Puget Lowland slightly northeast of the Olympic Mountains, and within the Cascadia subduction zone forearc where oblique convergence causes active structures to accommodate shortening (Johnson and others, 2004; McCaffrey and others, 2007). The regionally prominent Olympic–Wallowa lineament (Raisz, 1945; Blakely and others, 2011) and most mapped faults within 10 mi of the map area all trend northwest (Fig. M1). Among these faults is the major, active, right-lateral transpressional southern Whidbey Island fault zone north, northeast, and east of the map area, which accommodates movement of southwestern Washington relative to North America (Gower, 1980; Johnson and others, 1996; Kelsey and others, 2004; Brocher and others, 2005; Sherrod and others, 2005a,b, 2008; Liberty and Pape, 2006; Blakely and others, 2011). South of the map area, the Dabob Bay fault zone (Blakely and others, 2009; Polenz and others, 2013; Contreras and others, 2014), is subparallel to, and may kinematically resemble, the southern Whidbey Island fault zone. In contrast, mapped faults in the map area trend northeast and east (Fig. M1). They may be relict structures, reflect complex tectonics that remain unexplained within the regional stress field, or indicate a locally divergent stress field; for instance, localized block rotation could result in complex local structures with ‘atypical’ orientations.

## STRUCTURAL INTERPRETATION OF THE MAP AREA

Like Yount and Gower (1991) and the authors of the adjacent Uncas and Port Townsend South 7.5-minute quadrangles (Tabor and others, 2011; Schasse and Slaughter, 2005), we find the structure in this area difficult to interpret. Geologic exposures in the Center quadrangle are sparse and typically limited to a few square feet. Many ‘exposures’ are so weathered that bedrock is difficult to recognize. Based on the available data, no single structural interpretation appears compelling, and the area is probably more tectonically complex than indicated by present mapping.

Measurements of bedding and joint orientations display considerable scatter. According to Tabor and Cady (1978), bedding surfaces include overturned bedrock at age site GD11 (sec. 17, T28N R1W). Bedrock exposures reveal a general trend from older bedrock near the northwestern map corner to progressively younger bedrock farther southeast, consistent with generally southeast-dipping bedding and the suspicion that the mostly northeast-trending faults include a component of vertical offset, but these trends do not continue north or southeast of the map area. Exposures of basalt between 0 and 5 mi east of the map area (Hanson, 1976; Grimstad and Carson, 1981; Yount and Gower, 1991; Contreras and others, 2013, and our own unpublished field notes) coincide with (and likely explain) elevated magnetic and gravity field strength and may be an expression of the Port Ludlow uplift (Fig. M1), but as Pratt and others (1997, p. 27,473) imply with their label “uplift of unknown origin”, the reason for this uplift is unclear. The unexplained uplift, scattered bedding orientations, uncertainty about the character and level of

activity of faults, and inability to project structural trends beyond the map area reinforce the sense that present mapping lacks a satisfactory tectonic model for and fails to capture the tectonic complexity of the area.

Tabor and others (2011) interpreted east dips of Crescent and Lyre Formation west of the Center quadrangle as evidence for post-late Eocene eastward tilting in response to growing Olympic Mountains uplift. The Center quadrangle is farther from the Olympic Mountains, and uplift of the Olympic Mountains southwest of the Center quadrangle provides no obvious rationale for east- to southeast-dipping bedding and northeast-striking faults in the Center quadrangle. Similarly, uplift of the Olympic Mountains does not explain the relatively elevated land area and widespread exposures of the oldest bedrock in the northwestern part of the quadrangle.

Available data within the map area seem insufficient to accept—or reject—the north–south shortening that Tabor and others (2011) inferred for sometime after deposition of the sandstone of Snow Creek in the adjacent Uncas quadrangle, but such shortening would be consistent with our speculation that an actively growing west-trending structure, or set of structures, deforms a 1-mi-wide swath along the northern map boundary (see *Evidence for Active Deformation*). Gower (1980) and Yount and Gower (1991) asserted that an angular unconformity separates steeply east-dipping Lyre Formation conglomerate from the overlying, gently east-dipping unit Tc (see *Bedrock Stratigraphy and Paleontology* and unit Em<sub>21c</sub>). We have insufficient bedding orientation data to confirm or refute the existence of this angular unconformity.

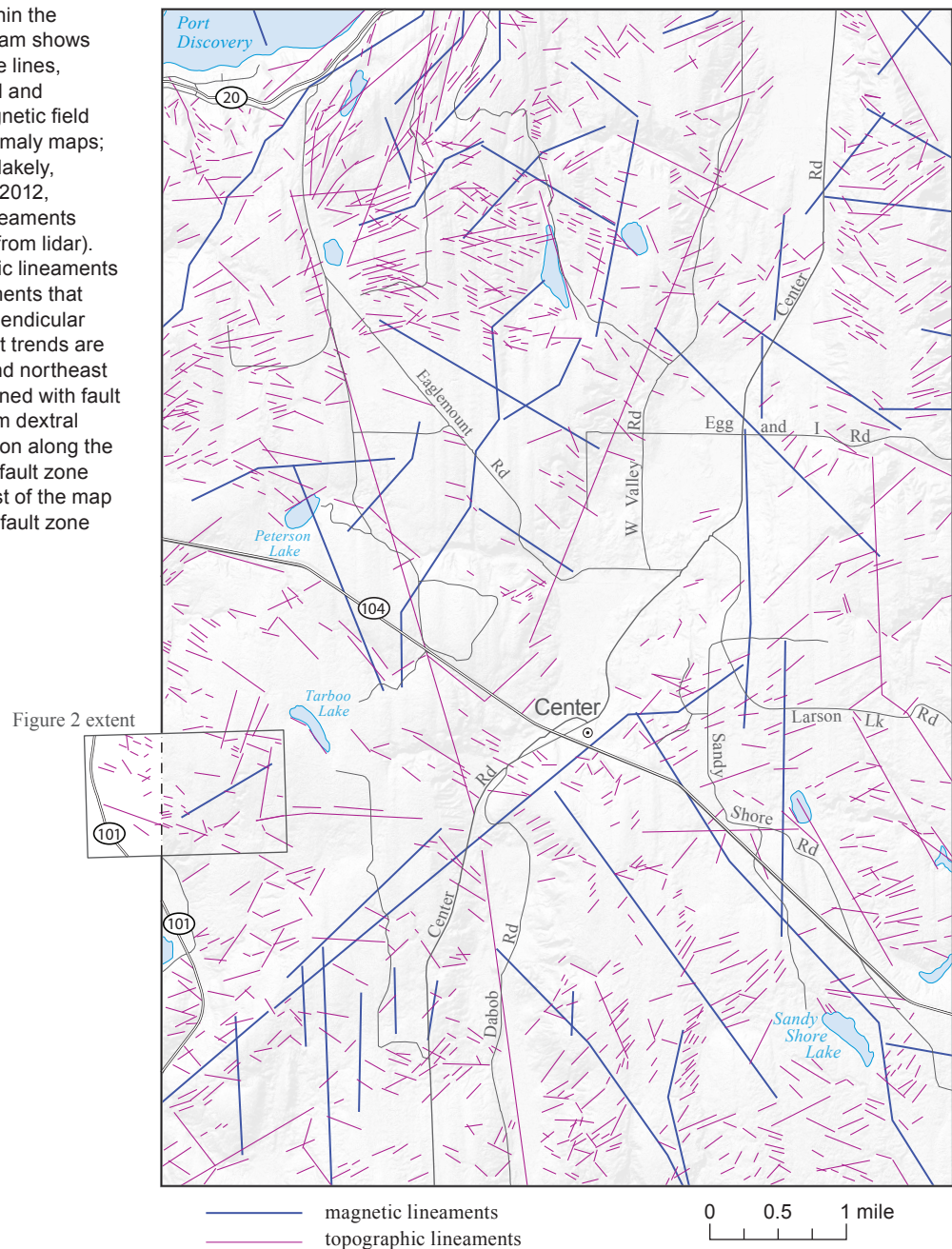
The apparent absence of Aldwell Formation in the map area suggests that the contact between the Crescent and Lyre Formations is unconformable (Haeussler and others, 1999; Tabor and others, 2011). Gower (1980) interpreted the contact between the two units as a fault. On the basis of the distribution of bedrock, presence of scarps and lineaments (magnetic and topographic), and Gower's mapping, we show most contacts between the Crescent and Lyre Formations as faulted but query these contacts because they may not require faulting. Faulted contacts between other units are similarly inspired by Gower (1980), who showed his faults as solid lines—for what reasons we do not know. We query our faults because we lack a convincing tectonic model for the map area. Nearly all the faults we show are inferred; without observed gouge, slickensides, or other definitive evidence of shear, a depositional unconformity, paleotopography, or differential erosion could alternatively explain the distribution of bedrock, scarps, and lineaments.

## Faults

Despite some very pronounced scarps and lineaments in the northwest quadrant of the map, we saw no fault that demonstrably cuts Quaternary deposits. We observed a clear fault exposure with gouge at only a single site, but that site lacks topographic lineaments and the fault there is flanked on both sides by sandstone of the same unit (Em<sub>1c</sub>) (short, west-striking, south-dipping, minor fault symbol in NW¼ sec. 21, T29N R1W). We did not see compelling evidence for other faults in the map area; however, we show several additional faults as inferred and queried. The inference of these faults is considerably inspired by Gower (1980) and Yount and Gower (1991), but locally modified from their fault alignments to better fit our field observations and lidar-based renderings of topography. Individual fault alignments are supported by scarps and lineaments, anomalies in the local magnetic gradient, chaotic bedding orientations near some strands, and observations of apparent stratigraphic gaps. One example is southeast of significant site S4 (sec. 36, T29N R2W), where pebble counts by Spencer (1984) document an elevated basalt-clast content that would suggest Lyre Formation basal conglomerate (unit Em<sub>21c</sub>) at the contact with overlying Lyre Formation sandstone (unit Em<sub>21s</sub>)—consistent with northwest-up offset. However, only slightly less basalt-rich clast counts obtained by Spencer at site S1 (sec. 30, T29N R1W) could be explained by either a northeast extension of the fault shown near site S4, or by a southwest extension of the southwest-trending, southeast-up(?) fault shown 1,500 ft northeast of site S1. Given the considerable scope for conflicting interpretations, we did not extend either fault. However, both could exist, and numerous southwest-trending topographic and several southwest-trending magnetic lineaments in the area may be unrecognized fault scarps. Some of the most prominent scarps and lineaments are shown on the map, but a more complete inventory (Fig. 1) would be incompatible with our 1:24,000-scale map. The faults shown on the map should therefore be viewed as illustration of a pattern of northeast- and east-trending faults in this area, but individual strands are more questionable than the overall pattern, and additional unrecognized strands are likely.

Most faults shown are adapted from Gower (1980) or Yount and Gower (1991), with modifications made to accommodate observed bedrock exposures and alignment of scarps and lineaments. We recognize that the fault distribution and characterization is not satisfactory and may not fit any internally coherent tectonic model. We do not believe that we have enough evidence to impose a tectonic model on the area and instead opted to show faults where we felt that evidence for faults was strongest and where map scale permitted their display. We

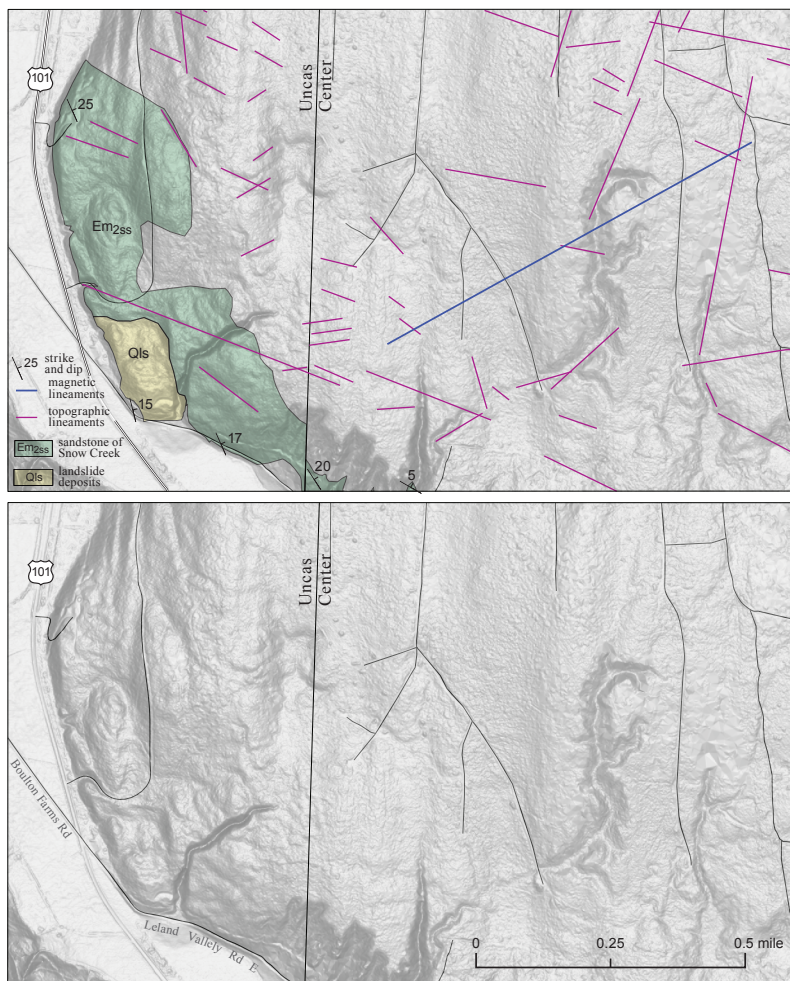
**Figure 1.** Lineaments within the Center quadrangle. Diagram shows magnetic lineaments (blue lines, interpreted from total-field and upward-migrated geomagnetic field strength and residual anomaly maps; maps courtesy Richard Blakely, USGS, written commun., 2012, 2013) and topographic lineaments (purple lines, interpreted from lidar). Compilation of topographic lineaments generally excludes lineaments that parallel fluting or are perpendicular to contours. The dominant trends are northwest to southeast and northeast to southwest, broadly aligned with fault orientations expected from dextral transpressional deformation along the southern Whidbey Island fault zone (north, northeast, and east of the map area) and the Dabob Bay fault zone (south of the map area).



strongly suspect that the area is more faulted than shown and hope that the faults we show at least are reasonably representative of structural patterns. The best evidence we observed for a compressional setting is a small-scale shear zone within basalt (N52°E–47°SE, with apparent southeast-up offset, unit Ev<sub>c</sub>) below SR 20 in the SW<sup>1</sup>/<sub>4</sub> sec. 19, T29N R2W. This assessment is tentative but consistent with the observed distribution of bedrock that supports the inferred reverse component of offset of the most westerly fault in Cross Section A–A' In contrast, the distribution of bedrock supports the normal component of offset shown for all other faults along that cross section. We have no information on the strike-slip component of the inferred faults. Faults not based on specific structures previously mapped by Gower (1980) or Yount and Gower (1991) still fit their pattern of northeast-striking faults and east-striking faults that may in places truncate the northeast-striking ones. All mapped faults are located in the northwest quarter of the map area where bedrock exposures are most widespread.

Not shown on Figure M1 (map sheet) is the north-striking Hood Canal fault (Daneš and others, 1965; Gower and others, 1985; Yount and Gower, 1991). Like Contreras and others (2014) and Polenz and others (2012, 2013), we

**Figure 2.** Lineaments near the border of the Center and Uncas quadrangles, 2.4 mi north of the southern map edge. Images show topographic and magnetic lineament trends from Figure 1, near area of concentrated epicenters in Figure 3. Landslide and bedrock areas obtained from mapping by Tabor and others (2011) in the Uncas quadrangle. Lineaments marked in the upper image were observed in multiple blended lidar hillshade renderings at various scales. We generally ignored lineaments that we perceived to be aligned with fluting, perpendicular to contours, or manmade (such as roads). Lower image omits coloration and lineaments for comparison. The identical composite hillshade images above are formed by using a slope shade and three hillshade images with simulated sun angles at 45 degrees above the horizon from the north, northeast, and northwest



omit that fault because we have little sense of its location or character in the map area and do not feel that it helps explain the character and distribution of known deposits or the Port Ludlow uplift inferred by Pratt and others (1997) east of the putative fault. However, an apparent north-trending bedrock trough beneath West Valley and Tarboo Creek is consistent with the presence of a Hood Canal fault (Cross Section A; Daniel Eungard, Wash. Div. of Geology and Earth Resources., written and oral commun., 2014).

### Other Structures

Although most bedrock in the map area is obviously folded, jointed, or tilted, available data do not support identification of specific folds at map scale. Cross Section A appears to show an anticline in the eastern third of the map area. We lack constraints on the mechanism(s) that led to shallow bedrock in this area and therefore do not show folds or bounding faults, though either or both may exist. The concave-down form of the bedrock depicted in Cross Section A is thus not meant to express an anticline (or absence thereof), but elevated magnetic and gravity field strengths suggest shallow basalt bedrock in the southeast quarter of the map area; this elevated bedrock roughly coincides with the Port Ludlow uplift (Fig. M1; Pratt and others, 1997). Unit Ev<sub>c</sub> is therefore shown schematically within 300 ft of the surface near the east end of Cross Section A, consistent with a western flank of the Port Ludlow uplift (that is separated from the basalt exposures east of the map area by a north-trending magnetic and gravity trough). Observations of sedimentary bedrock 2.3 mi northeast of the cross section (0.2–0.7 mi east of the map area) suggest that the basalt in the map area may be draped by sedimentary bedrock; units Em<sub>1c</sub> and ØEm are thus shown (schematically) above unit Ev<sub>c</sub>. The evidence for the sedimentary bedrock units here is clearly speculative, and the thickness shown is inexplicably thinner than the same units farther west along the cross section. Thinner (or absent) sedimentary rock units were needed, however to permit basalt bedrock to approach the surface, as is suggested by the high gravity and magnetic field strength.

### *Evidence for Active Deformation*

The coincidence of multiple observations, each of which would be unremarkable in isolation, suggests that a west-trending anticline or (and?) fault-bounded structural high may be developing about 0.5 mi south of the northern map edge. In West Valley, a west-trending, gentle saddle of sand (unit Qgos) rises about 5 ft above the surrounding peat or muck-covered valley floor (unit Qp) between 0.25 and 0.45 mi south of the northern map edge (significant site S3, sec. 23, T29N R1W). At peat survey line Rigg C (map sheet, 0.5 mi south of site S3), Rigg (1958) documented as much as 44 ft of peat, and interpreted a tephra layer 30 ft below the peat surface as the 6,000-yr-old Glacier Peak deposit (Rigg and Gould, 1957). In Chimacum Valley at peat survey line Rigg A (0.8 mi east of S3), Rigg (1958) documented 9 ft of peat and identified the same tephra within peat 1 to 4 ft below the surface.

The absence of peat at site S3 implies that this part of the valley floor has stood above areas to the north and south since the onset of muck and peat formation. If Rigg's identification of 6,000-yr-old tephra is correct, it implies nearly 50 ft of sedimentary valley floor relief (below the peat) between site S3 and Rigg C, and that the upper 30 ft of peat at Rigg C formed after 6,000 yrs ago. One way to interpret this is that post-glacial valley floor deformation elevated S3 above the surrounding valley floor and impounded a lake at Rigg C. A simpler interpretation may be that the relief between site S3 and Rigg C was already present and impounding a lake at Rigg C at the end of the Vashon Stade, and that Pleistocene to early Holocene lake floor sedimentation filled in the lake and led to late Holocene peat formation, without post-glacial valley floor deformation. This interpretation is consistent with our speculation that Everson Interstade meltwater discharge to Adelma Beach (4 mi north of the map area) was fed chiefly from Chimacum Valley, with outwash sedimentation in West Valley resulting mainly from coeval slackwater inundation (see also *Glacial Lakes, Shorelines, and Everson Interstade Marine Incursion*). If correct, this suggests that the Chimacum Valley floor should form a more consistent north-down slope than the floor of West Valley, unless Chimacum Valley meltwater discharge was subglacial. Rigg's documentation of peat at Rigg A in Chimacum Valley with the putative 6,000-yr-old tephra within 5 ft of the surface is consistent with that interpretation but would also permit post-glacial relative uplift of the valley floor at both site S3 and Rigg A.

A gravel excavation at site S7 (1.7 mi southwest of the northeastern map corner) reveals some minor faults in gravel. It is unclear if these penetrate to the surface and whether their origin is due to ice shove, but they would be consistent with a west-trending, growing structure in this area.

A wetland in a flat-bottomed basin (mapped as unit Qp) at significant site S2 (sec. 22, T29N R1W, 1 mi west of S3) is crossed by a 2-to 3-ft-deep creek. Orthophotos indicate that the channel meanders within a straight, 500-ft-long and 50-ft-wide, east-trending corridor and has not appreciably changed alignment in at least 11 years (2000–2011). We find the observed straight drainage across this peat bog to be unique. One possible explanation for this unusual feature would be on-going growth of a west-trending fold across the wetland. If so, this fold would be aligned with—and perhaps related to—the sand ledge across West Valley at site S3.

Between 0.7 and 1 mi west of site S2, we used bedrock distribution to infer two parallel, west-trending faults that together raise the land between them above that to the north and south. Their location and sense of offset would be consistent with active land-level change along a western extension of the axis of possible west-trending folding at significant sites S2 and S3. If the same westerly trend is extended 4 mi west from site S2 across the rest of the map area and beyond, it meets Port Discovery at the mouth of Uncas Creek, where US 101 crosses the creek. The onset of dry land at that latitude may be unrelated, but its alignment with other elevated regions is at least consistent with an actively growing, west-trending fold, perhaps bounded by the faults recognized 0.7 to 1 mi west of site S2.

### **Seismicity**

Mace and Keranen (2012) observed that much of the crustal seismicity beneath the Puget Lowland is not explained by mapped faults. This pattern applies to the Center quadrangle and some nearby areas. A concentration of (instrumentally) recorded crustal earthquake epicenters near the southern margin of the map area (Fig. 3) suggests that the Lofall fault (Contreras and others, 2013) might project west-northwest across the quadrangle. Many lineaments not aligned with bedding orientations, nor explained by fluting or slope aspect, also are consistent with west-northwest-trending structure(s) across the map area (Fig. M1; Figs. 1 and 2). Along the western map edge near the southwest map corner, a landslide headscarp is tangent to one of the strongest lineaments (Fig. 2), consistent with fault control of the headscarp. However, magnetic lineaments and gravity anomalies do not align with a hypothetical western extension of the Lofall fault, and most of the 14 crustal earthquake focal mechanisms near the southwest map corner instead suggest northeast-trending compressional faulting (Fig. B1; Table B1).

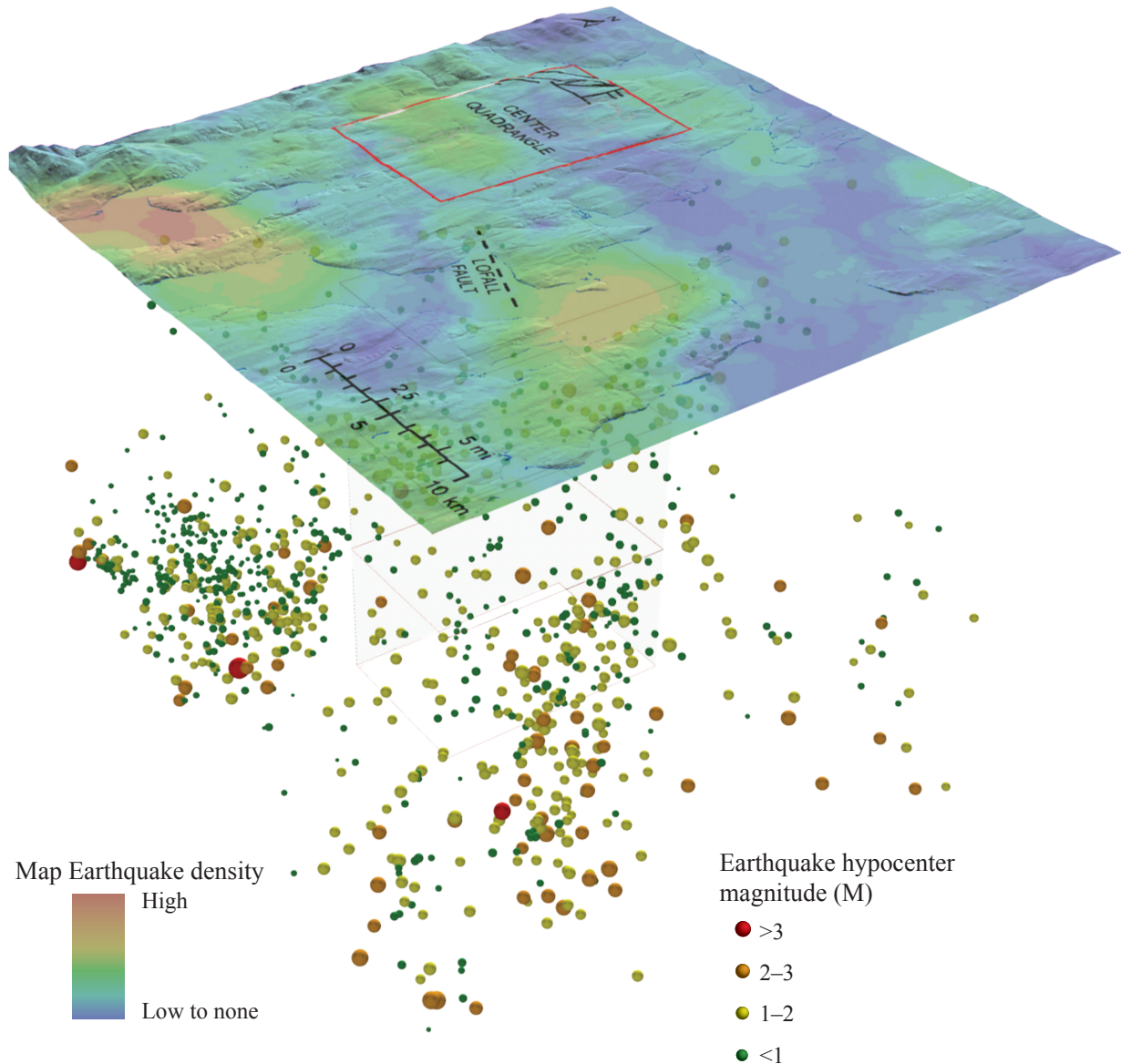


**Figure 3.** Three-dimensional rendering of earthquake locations beneath the Center quadrangle and vicinity. View angle is to the northwest. Clicking on the image above will open a rotatable 3D graphic in your web browser. Red rectangle outlines the Center quadrangle. The gray rectangular pillar shades the subsurface beneath the quadrangle —rectangles mark 5, 10, 15, and 20 mi depths. Data were obtained March 5, 2014, from the Pacific Northwest Seismic Network ([www.pnsn.org](http://www.pnsn.org)) and include all seismic events with focal depths less than 20 mi that occurred between  $-122.2$  and  $-123.05^\circ$  latitude and  $47.6$  to  $48.2^\circ$  longitude from 1970 to March 5, 2014, except for a cluster of near-surface tremors 1 to 2 mi east of the southeast boundary of the Center quadrangle that we interpreted as quarry blasts. These shallow tremors were also excluded from the calculation of a (two-dimensional) earthquake epicenter density grid, represented by the color of hillshade. The earthquake hypocenters shown in the figure also exclude several near-surface ( $<0.1$  mi depth) earthquakes that, due to scale issues, could not be shown below the topographic surface of the image, as well as several hypocenters that could not be properly projected in the available 3D software. Of the 1,089 seismic events represented in the image, 94 are beneath the Center quadrangle. Most events imaged between the southwest and northeast quadrangle corners are east of the map area (between the viewer and the quadrangle), and of the 94 beneath the quadrangle, nearly all are beneath the south half. Topography is rendered from lidar-based elevation data, with no vertical exaggeration. Mapped faults within the Center quadrangle, shown as solid black lines, are from the map sheet. Outside the map area, only the Lofall fault (Contreras and others, 2013) is shown (dashed black line).

If our interpreted orientations and compressional character of north-northeast-trending surficial faults in the northwest quarter of the map area are correct, the strain from those faults resembles that of recorded deeper crustal earthquakes near the southwest map corner. In addition, many topographic and magnetic lineaments also trend northeast, including lineaments around both the southwest map corner and the mapped surficial faults near the northwest map corner (Figs. 1 and 2). However, all but two of the 66 seismic events with focal mechanisms are deeper than 13 km (8 mi) (Table B1), such that a link between the recorded seismicity and structures at the surface is not established. The observed earthquakes therefore could represent faulting only beneath the upper crust—perhaps along boundaries between blocks of basaltic and sedimentary bedrock below the Puget Sound thrust sheet of Pratt and others (1997); any connection to surficial faulting is questionable.

## ACKNOWLEDGMENTS

This geologic map was funded in part by the USGS National Cooperative Geologic Mapping Program under award no. G13AC00173. We thank Jeff Tepper (Univ. of Puget Sound) for assistance with field observations, thin section petrographic sample analysis, geochemistry, interpretation, and assistance with writing and other tasks; Shannon Mahan and Harrison Gray (USGS) for analysis of luminescence samples; Elizabeth Nesbitt (Burke Museum, Univ. of Wash.) for assistance with bedrock fossil content and ages; the Jefferson County Assessor's Office for GIS data; the Wash. State Dept. of Transportation for access to geotechnical records and Eric Dingeldein for his assistance with those records; Rex Crawford, Joe Arnett, and Joe Rocchio (all WADNR Natural Heritage Program) for assistance with organic sample species identification; Richard Blakely (USGS) for aeromagnetic field strength maps; Andy Lamb (USGS) for magnetic, gravity, seismic line, and other data; Bob Carson (Whitman College) and Kathryn Hanson (AMEC) for sharing their field notes and knowledge of the area; Daniel Eungard (DGER) for assistance with three-dimensional graphic imaging of geospatial data; and George Kwok and Grady Olson for field help. We thank countless landowners for sharing local knowledge and permitting us to map on their land.

## REFERENCES CITED

- Allison, R. C., 1959, The geology and Eocene megafaunal paleontology of the Quimper Peninsula area, Washington: University of Washington Master of Science thesis, 121 p., 1 plate.
- Anundsen, Karl; Abella, S. E. B.; Leopold, E. B.; Stuiver, M.; Turner, S., 1994, Late-glacial and early Holocene sea-level fluctuations in the central Puget Lowland, Washington, inferred from lake sediments: *Quaternary Research*, v. 42, no. 2, p. 149-161.
- Arnold, Ralph, 1906, Geological reconnaissance of the coast of the Olympic Peninsula, Washington: *Geological Society of America Bulletin*, v. 17, p. 451-468.
- Babcock, R. S.; Burmester, R. F.; Engebretson, D. C.; Warnock, A. C.; Clark, K. P., 1992, A rifted margin origin for the Crescent basalts and related rocks in the northern Coast Range volcanic province, Washington and British Columbia: *Journal of Geophysical Research*, v. 97, no. B5, p. 6799-6821.
- Babcock, R. S.; Suczek, C. A.; Engebretson, D. C., 1994, The Crescent "terrane", Olympic Peninsula and southern Vancouver Island. *In* Lasmanis, Raymond; Cheney, E. S., convenors, *Regional geology of Washington State: Washington Division of Geology and Earth Resources Bulletin 80*, p. 141-157. [[http://www.dnr.wa.gov/publications/ger\\_b80\\_regional\\_geol\\_wa\\_2.pdf](http://www.dnr.wa.gov/publications/ger_b80_regional_geol_wa_2.pdf)]
- Blakely, R. J.; Sherrod, B. L.; Hughes, J. F.; Anderson, M. L.; Wells, R. E.; Weaver, C. S., 2009, Saddle Mountain fault deformation zone, Olympic Peninsula, Washington—Western boundary of the Seattle uplift: *Geosphere*, v. 5, no. 2, p. 105-125.
- Blakely, R. J.; Sherrod, B. L.; Weaver, C. S.; Wells, R. E.; Rohay, A. C.; Barnett, E. A.; Knepprath, N. E., 2011, Connecting the Yakima fold and thrust belt to active faults in the Puget Lowland, Washington: *Journal of Geophysical Research*, v. 116, B07105, 33 p.
- Booth, D. B., 1994, Glaciofluvial infilling and scour of the Puget Lowland, Washington, during ice-sheet glaciation: *Geology*, v. 22, no. 8, p. 695-698.
- Booth, D. B.; Troost, K. G.; Clague, J. J.; Waitt, R. B., 2004, The Cordilleran ice sheet. *In* Gillespie, A. R.; Porter, S. C.; Atwater, B. F., editors, *The Quaternary period in the United States*: Elsevier, p. 17-43.
- Bowman, J. D.; Czajkowski, J. L., 2013, Washington State seismogenic features database [GIS data]: Washington Division of Geology and Earth Resources Digital Data Series DS-1, version 3.0. [[http://www.dnr.wa.gov/publications/ger\\_portal\\_seismogenic\\_features.zip](http://www.dnr.wa.gov/publications/ger_portal_seismogenic_features.zip)]

- Bretz, J. H., 1910, Glacial lakes of Puget Sound—Preliminary paper: *Journal of Geology*, v. 18, no. 5, p. 448-458.
- Bretz, J. H., 1913, Glaciation of the Puget Sound region: *Washington Geological Survey Bulletin* 8, 244 p., 3 plates. [[http://www.dnr.wa.gov/publications/ger\\_b8\\_glaciation\\_pugetsound.pdf](http://www.dnr.wa.gov/publications/ger_b8_glaciation_pugetsound.pdf)]
- Brocher, T. M.; Blakely, R. J.; Wells, R. E.; Sherrod, B. L.; Ramachandran, Kumar, 2005, The transition between N-S and NE-SW directed crustal shortening in the central and northern Puget Lowland—New thoughts on the southern Whidbey Island fault [abstract]: *Eos (American Geophysical Union Transactions)*, v. 86, no. 52, p. F1459.
- Brown, R. D., Jr.; Gower, H. D.; Snively, P. D., Jr., 1960, Geology of the Port Angeles–Lake Crescent area, Clallam County, Washington: U.S. Geological Survey Oil and Gas Investigations Map OM-203, 1 sheet, scale 1:62,500. [[http://ngmdb.usgs.gov/Prodesc/proddesc\\_5357.htm](http://ngmdb.usgs.gov/Prodesc/proddesc_5357.htm)]
- Brown, R. D., Jr.; Snively, P. D., Jr.; Gower, H. D., 1956, Lyre formation (redefinition), northern Olympic Peninsula, Washington: *American Association of Petroleum Geologists Bulletin*, v. 40, no. 1, p. 94-107.
- Cady, W. M.; Sorensen, M. L.; MacLeod, N. S., 1972a, Geologic map of the Brothers quadrangle, Jefferson, Mason and Kitsap Counties, Washington: U.S. Geological Survey Geologic Quadrangle Map GQ-969, 1 sheet, scale 1:62,500. [<http://pubs.usgs.gov/gq/0969/report.pdf>]
- Cady, W. M.; Tabor, R. W.; MacLeod, N. S.; Sorensen, M. L., 1972b, Geologic map of the Tyler Peak quadrangle, Clallam and Jefferson Counties, Washington: U.S. Geological Survey Geologic Quadrangle Map GQ-970, 1 sheet, scale 1:62,500. [<http://pubs.usgs.gov/gq/0970/report.pdf>]
- Contreras, T. A.; Patton, A. I.; Legoretta Paulin, Gabriel; Cakir, Recep; Carson, R. J., 2014, Geologic map of the Quilcene 7.5-minute quadrangle, Jefferson County, Washington: Washington Division of Geology and Earth Resources Map Series 2014-03, 1 sheet, scale 1:24,000, with 28 p. text. [[http://www.dnr.wa.gov/publications/ger\\_ms2014-03\\_geol\\_map\\_quilcene\\_24k.zip](http://www.dnr.wa.gov/publications/ger_ms2014-03_geol_map_quilcene_24k.zip)]
- Contreras, T. A.; Spangler, Eleanor; Fusso, L. A.; Reioux, D. A.; Legorreta Paulin, Gabriel; Pringle, P. T.; Carson, R. J.; Lindstrum, E. F.; Clark, K. P.; Tepper, J. H.; Pileggi, Domenico; Mahan, S. A., 2012a, Geologic map of the Eldon 7.5-minute quadrangle, Jefferson, Kitsap, and Mason Counties, Washington: Washington Division of Geology and Earth Resources Map Series 2012-03, 1 sheet, scale 1:24,000, 60 p. text. [[http://www.dnr.wa.gov/publications/ger\\_ms2012-03\\_geol\\_map\\_eldon\\_24k.zip](http://www.dnr.wa.gov/publications/ger_ms2012-03_geol_map_eldon_24k.zip)]
- Contreras, T. A.; Stone, K. A.; Legorreta Paulin, Gabriel, 2013, Geologic map of the Lofall 7.5-minute quadrangle, Jefferson and Kitsap Counties, Washington: Washington Division of Geology and Earth Resources Map Series 2013-03, 1 sheet, scale 1:24,000, with 19 p. text. [[http://www.dnr.wa.gov/publications/ger\\_ms2013-03\\_geol\\_map\\_lofall\\_24k.zip](http://www.dnr.wa.gov/publications/ger_ms2013-03_geol_map_lofall_24k.zip)]
- Contreras, T. A.; Weeks, S. A.; Perry, B. B., 2012b, Analytical data from the Holly 7.5-minute quadrangle, Jefferson, Kitsap, and Mason Counties, Washington—Supplement to Open File Report 2011-5: Washington Division of Geology and Earth Resources Open File Report 2011-6, 16 p. [[http://www.dnr.wa.gov/publications/ger\\_ofr2011-6\\_holly\\_supplement.pdf](http://www.dnr.wa.gov/publications/ger_ofr2011-6_holly_supplement.pdf)]
- Contreras, T. A.; Weeks, S. A.; Stanton, K. M. D.; Stanton, B. W.; Perry, B. B.; Walsh, T. J.; Carson, R. J.; Clark, K. P.; Mahan, S. A., 2012c, Geologic map of the Holly 7.5-minute quadrangle, Jefferson, Kitsap, and Mason Counties, Washington: Washington Division of Geology and Earth Resources Open File Report 2011-5, 1 sheet, scale 1:24,000, with 13 p. text. [[http://www.dnr.wa.gov/publications/ger\\_ofr2011-5\\_geol\\_map\\_holly\\_24k.zip](http://www.dnr.wa.gov/publications/ger_ofr2011-5_geol_map_holly_24k.zip)]
- Daneš, Z. F.; Bonno, M.; Brau, J. E.; Gilham, W. D.; Hoffman, T. F.; Johansen, D.; Jones, M. H.; Malfait, Bruce; Masten, J.; Teague, G. O., 1965, Geophysical investigation of the southern Puget Sound area, Washington: *Journal of Geophysical Research*, v. 70, no. 22, p. 5573-5580.
- Deeter, J. D., 1979, Quaternary geology and stratigraphy of Kitsap County, Washington: Western Washington University Master of Science thesis, 175 p., 1 plate, scale 1:42,000.
- Defant, M. J.; Drummond, M. S., 1990, Derivation of some modern arc magmas by melting of young subducted lithosphere: *Nature*, v. 347, p. 662-665.
- Dethier, D. P.; Pessl, Fred, Jr.; Keuler, R. F.; Balzarini, M. A.; Pevear, D. R., 1995, Late Wisconsinan glaciomarine deposition and isostatic rebound, northern Puget Lowland, Washington: *Geological Society of America Bulletin*, v. 107, no. 11, p. 1288-1303.
- Dragovich, J. D.; Logan, R. L.; Schasse, H. W.; Walsh, T. J.; Lingley, W. S., Jr.; Norman, D. K.; Gerstel, W. J.; Lapen, T. J.; Schuster, J. E.; Meyers, K. D., 2002, Geologic map of Washington—Northwest quadrant: Washington Division of Geology and Earth Resources Geologic Map GM-50, 3 sheets, scale 1:250,000, with 72 p. text. [[http://www.dnr.wa.gov/publications/ger\\_gm50\\_geol\\_map\\_nw\\_wa\\_250k.pdf](http://www.dnr.wa.gov/publications/ger_gm50_geol_map_nw_wa_250k.pdf)]
- Dragovich, J. D.; Pringle, P. T.; Walsh, T. J., 1994, Extent and geometry of the mid-Holocene Osceola mudflow in the Puget Lowland—Implications for Holocene sedimentation and paleogeography: *Washington Geology*, v. 22, no. 3, p. 3-26. [[http://www.dnr.wa.gov/publications/ger\\_washington\\_geology\\_1994\\_v22\\_no3.pdf](http://www.dnr.wa.gov/publications/ger_washington_geology_1994_v22_no3.pdf)]
- Durham, J. W., 1944, Megafaunal zones of the Oligocene of northwestern Washington: *University of California Department of Geological Sciences Bulletin*, v. 27, no. 5, p. 101-212.

- Eronen, Matti; Kankainen, Tuovi; Tsukada, Matsuo, 1987, Late Holocene sea-level record in a core from the Puget Lowland, Washington: *Quaternary Research*, v. 27, no. 2, p. 147-159.
- Gayer, M. J., 1976, Geologic map of northeastern Jefferson County, Washington: Washington Division of Geology and Earth Resources Open File Report 76-21, 1 sheet, scale 1:24,000. [[http://www.dnr.wa.gov/publications/ger\\_ofr76\\_21\\_geol\\_map\\_jefferson\\_co\\_24k.pdf](http://www.dnr.wa.gov/publications/ger_ofr76_21_geol_map_jefferson_co_24k.pdf)]
- Gayer, M. J., 1977, Quaternary and environmental geology of northeastern Jefferson County, Washington: North Carolina State University Master of Science thesis, 140 p.
- Glassley, W. E., 1974, Geochemistry and tectonics of the Crescent volcanic rocks, Olympic Peninsula, Washington: *Geological Society of America Bulletin*, v. 85, no. 5, p. 785-794.
- Gower, H. D., 1980, Bedrock geologic and Quaternary tectonic map of the Port Townsend area, Washington: U.S. Geological Survey Open-File Report 80-1174, 1 sheet, scale 1:100,000, with 19 p. text. [<http://pubs.er.usgs.gov/usgspubs/ofr/ofr801174>]
- Gower, H. D.; Yount, J. C.; Crosson, R. S., 1985, Seismotectonic map of the Puget Sound region, Washington: U.S. Geological Survey Miscellaneous Investigations Series Map I-1613, 1 sheet, scale 1:250,000, with 15 p. text. [<http://pubs.usgs.gov/imap/1613/plate-1.pdf>]
- Grimstad, Peder; Carson, R. J., 1981, Geology and ground-water resources of eastern Jefferson County, Washington: Washington Department of Ecology Water-Supply Bulletin 54, 125 p., 3 plates. [[http://www.ecy.wa.gov/programs/eap/wsb/wsb\\_All.html](http://www.ecy.wa.gov/programs/eap/wsb/wsb_All.html)]
- Haessler, P. J.; Yount, J. C.; Wells, R. E., 1999, Preliminary geologic map of the Uncas 7.5' quadrangle, Clallam and Jefferson Counties, Washington: U.S. Geological Survey Open-File Report 99-421, 1 sheet, scale 1:24,000. [<http://pubs.er.usgs.gov/usgspubs/ofr/ofr99421>]
- Hahn, M.; Graetinger, A.; Gustafson, J.; Ponzini, C.; Wolfe, M.; Peters, R.; Stein, K.; Tepper, J., 2004, Eocene pyroclastic deposits at Chimacum, Washington—Adakite magmatism in the Cascadia forearc [abstract]: *Geological Society of America Abstracts with Programs*, v. 36, no. 4, p. 69.
- Hanson, K. L., 1976, Geologic map of the Uncas–Port Ludlow area, Jefferson County, Washington: Washington Division of Geology and Earth Resources Open File Report 76-20, 1 sheet, scale 1:24,000. [[http://www.dnr.wa.gov/publications/ger\\_ofr76-20\\_geol\\_map\\_uncas\\_port\\_ludlow\\_24k.pdf](http://www.dnr.wa.gov/publications/ger_ofr76-20_geol_map_uncas_port_ludlow_24k.pdf)]
- Haugerud, R. A., 2009, Preliminary geomorphic map of the Kitsap Peninsula, Washington: U.S. Geological Survey, Open-File Report 2009-1033, 2 sheets, scale 1:36,000. [<http://pubs.usgs.gov/of/2009/1033/>]
- Hirsch, D. M.; Babcock, R. S., 2009, Spatially heterogeneous burial and high-P/T metamorphism in the Crescent Formation, Olympic Peninsula, Washington: *American Mineralogist*, v. 94, no. 8-9, p. 1103-1110.
- Jillson, W. R., 1915, A preliminary report on the stratigraphy and the paleontology of the Quimper Peninsula of the State of Washington: University of Washington Master of Science thesis, 65 p., 1 plate.
- Johnson, S. Y.; Blakely, R. J.; Stephenson, W. J.; Dadisman, S. V.; Fisher, M. A., 2004, Active shortening of the Cascadia forearc and implications for seismic hazards of the Puget Lowland: *Tectonics*, v. 23, TC1011, doi:10.1029/2003TC001507, 2004, 27 p.
- Johnson, S. Y.; Potter, C. J.; Armentrout, J. M.; Miller, J. J.; Finn, C. A.; Weaver, C. S., 1996, The southern Whidbey Island fault—An active structure in the Puget Lowland, Washington: *Geological Society of America Bulletin*, v. 108, no. 3, p. 334-354, 1 plate.
- Kelsey, H. M.; Sherrod, Brian; Johnson, S. Y.; Dadisman, S. V., 2004, Land-level changes from a late Holocene earthquake in the northern Puget Lowland, Washington: *Geology*, v. 32, no. 6, p. 469-472.
- Laprade, W. T., 2003, Subglacially reworked till in the Puget Lowland [abstract]: *Geological Society of America Abstracts with Programs*, v. 35, no. 6, p. 216.
- Le Bas, M. J.; Le Maitre, R.W.; Streckeisen, A.; Zanettin, B., 1986, A chemical classification of volcanic rocks based on the total alkali silica diagram: *Journal of Petrology*, v. 27, p. 745-750.
- Lees, J. M., 2007, RFOC—Graphics for spherical distributions and earthquake focal mechanisms, graphics for statistics on a sphere, as applied to geological fault data, crystallography, earthquake focal mechanisms, radiation patterns, ternary plots and geographical/geological maps: Comprehensive R Archive Network (CRAN). [accessed May 31, 2011, at <http://streaming.stat.iastate.edu/CRAN/web/packages/RFOC/index.html>].
- Liberty, L. M.; Pape, K. M., 2006, Seismic characterization of the Seattle and southern Whidbey Island fault zones in the Snoqualmie River valley, Washington—Final technical report: U.S. Geological Survey Earthquake Hazards Program, External Research Support, Funded Research Final Technical Reports, 17 p. [<http://earthquake.usgs.gov/research/external/reports/06HQGR0111.pdf>]
- Mace, C. G.; Keranen, K. M., 2012, Oblique fault systems crossing the Seattle basin—Geophysical evidence for additional shallow fault systems in the central Puget Lowland: *Journal of Geophysical Research*, v. 117, B03105, 19 p.

- Martin, H.; Smithies, R. H.; Rapp, R.; Moyen, J. F.; Champion, D., 2005, An overview of adakite, tonalite–trondhjemite–granodiorite (TTG), and sanukitoid—relationships and some implications for crustal evolution: *Lithos* v. 79, p. 1-24.
- McCaffrey, Robert; Qamar, A. I.; King, R. W.; Wells, Ray; Khazaradze, Giorgi; Williams, C. A.; Stevens, C. W.; Vollick, J. J.; Zwick, P. C., 2007, Fault locking, block rotation and crustal deformation in the Pacific Northwest: *Geophysical Journal International*, v. 169, no. 3, p. 1315-1340.
- McDougall, Kristin, 2007, California Cenozoic biostratigraphy—Paleogene. *In* Hosford Scheirer, Allegra, editor, 2007, Petroleum systems and geologic assessment of oil and gas in the San Joaquin Basin Province, California: U.S. Geological Survey Professional Paper 1713. [<http://pubs.usgs.gov/pp/pp1713/>]
- McMichael, L. B., 1946, Geology of the northeastern Olympic Peninsula: University of Washington Master of Science thesis, 33 p., 1 plate.
- Morrison, R. B., 1991, Introduction. *In* Morrison, R. B., editor, Quaternary nonglacial geology—Conterminous U.S.: Geological Society of America DNAG Geology of North America, v. K-2, p. 1-12.
- Mosher, D. C.; Hewitt, A. T., 2004, Late Quaternary deglaciation and sea-level history of eastern Juan de Fuca Strait, Cascadia: *Quaternary International*, v. 121, no. 1, p. 23-39.
- Mullen, E. D., 1983, MnO/TiO<sub>2</sub>/P<sub>2</sub>O<sub>5</sub>—A minor element discriminant for basaltic rocks of oceanic environments and its implications for petrogenesis: *Earth and Planetary Science Letters*, v. 62, p. 53-62.
- Pettijohn, F. J., 1957, Sedimentary rocks: Harper and Brothers, 718 p.
- Polenz, Michael; Alldritt, Katelin; Heheman, N. J.; Logan, R. L., 2009a, Geologic map of the Burley 7.5-minute quadrangle, Kitsap and Pierce Counties, Washington: Washington Division of Geology and Earth Resources Open File Report 2009-8, 1 sheet, scale 1:24,000. [[http://www.dnr.wa.gov/publications/ger\\_ofr2009-8\\_geol\\_map\\_burley\\_24k.pdf](http://www.dnr.wa.gov/publications/ger_ofr2009-8_geol_map_burley_24k.pdf)]
- Polenz, Michael; Alldritt, Katelin; Heheman, N. J.; Sarikhan, I. Y.; Logan, R. L., 2009b, Geologic map of the Belfair 7.5-minute quadrangle, Mason, Kitsap, and Pierce Counties, Washington: Washington Division of Geology and Earth Resources Open File Report 2009-7, 1 sheet, scale 1:24,000. [[http://www.dnr.wa.gov/publications/ger\\_ofr2009-7\\_geol\\_map\\_belfair\\_24k.pdf](http://www.dnr.wa.gov/publications/ger_ofr2009-7_geol_map_belfair_24k.pdf)]
- Polenz, Michael; Contreras, T. A.; Czajkowski, J. L.; Legorreta Paulín, Gabriel; Miller, B. A.; Martin, M. E.; Walsh, T. J.; Logan, R. L.; Carson, R. J.; Johnson, C. N.; Skov, R. H.; Mahan, S. A.; Cohan, C. R., 2010, Supplement to geologic maps of the Lilliwaup, Skokomish Valley, and Union 7.5-minute quadrangles, Mason County, Washington—Geologic setting and development around the Great Bend of Hood Canal: Washington Division of Geology and Earth Resources Open File Report 2010-5, 27 p. [[http://www.dnr.wa.gov/publications/ger\\_ofr2010-5\\_lilliwaup\\_skokomish\\_valley\\_union\\_suppl\\_24k.pdf](http://www.dnr.wa.gov/publications/ger_ofr2010-5_lilliwaup_skokomish_valley_union_suppl_24k.pdf)]
- Polenz, Michael; Czajkowski, J. L.; Legorreta Paulín, Gabriel; Contreras, T. A.; Miller, B. A.; Martin, M. E.; Walsh, T. J.; Logan, R. L.; Carson, R. J.; Johnson, C. N.; Skov, R. H.; Mahan, S. A.; Cohan, C. R., 2011, Geologic map of the Skokomish Valley and Union 7.5-minute quadrangles, Mason County, Washington: Washington Division of Geology and Earth Resources Open File Report 2010-3 revised, 21 p., 1 plate, scale 1:24,000. [[http://www.dnr.wa.gov/publications/ger\\_ofr2010-3\\_geol\\_map\\_skokomish\\_valley\\_union\\_24k.zip](http://www.dnr.wa.gov/publications/ger_ofr2010-3_geol_map_skokomish_valley_union_24k.zip)]
- Polenz, Michael; Miller, B. A.; Davies, Nigel; Perry, B. B.; Clark, K. P.; Walsh, T. J.; Carson, R. J.; Hughes, J. F., 2012a, Geologic map of the Hoodspout 7.5-minute quadrangle, Mason County, Washington: Washington Division of Geology and Earth Resources Open File Report 2011-3, 1 sheet, scale 1:24,000, with 16 p. text. [[http://www.dnr.wa.gov/publications/ger\\_ofr2011-3\\_geol\\_map\\_hoodspout\\_24k.zip](http://www.dnr.wa.gov/publications/ger_ofr2011-3_geol_map_hoodspout_24k.zip)]
- Polenz, Michael; Miller, B. A.; Davies, Nigel; Perry, B. B.; Hughes, J. F.; Clark, K. P.; Walsh, T. J.; Tepper, J. H.; Carson, R. J., 2012b, Analytical data from the Hoodspout 7.5-minute quadrangle, Mason County, Washington—Supplement to Open File Report 2011-3: Washington Division of Geology and Earth Resources Open File Report 2011-4, 42 p. [[http://www.dnr.wa.gov/publications/ger\\_ofr2011-4\\_hoodspout\\_supplement.pdf](http://www.dnr.wa.gov/publications/ger_ofr2011-4_hoodspout_supplement.pdf)]
- Polenz, Michael; Petro, G. T.; Contreras, T. A.; Stone, K. A.; Legorreta Paulín, Gabriel; Cakir, Recep, 2013, Geologic map of the Seabeck and Poulsbo 7.5-minute quadrangles, Kitsap and Jefferson Counties, Washington: Washington Division of Geology and Earth Resources Map Series 2013-02, 1 sheet, scale 1:24,000, with 39 p. text. [[http://www.dnr.wa.gov/publications/ger\\_ms2013-02\\_geol\\_map\\_seabeck-poulsbo\\_24k.zip](http://www.dnr.wa.gov/publications/ger_ms2013-02_geol_map_seabeck-poulsbo_24k.zip)]
- Polenz, Michael; Spangler, Eleanor; Fusso, L. A.; Reieux, D. A.; Cole, R. A.; Walsh, T. J.; Cakir, Recep; Clark, K. P.; Tepper, J. H.; Carson, R. J.; Pileggi, Domenico; Mahan, S. A., 2012c, Geologic map of the Brinnon 7.5-minute quadrangle, Jefferson and Kitsap Counties, Washington: Washington Division of Geology and Earth Resources Map Series 2012-02, 1 sheet, scale 1:24,000, with 47 p. text. [[http://www.dnr.wa.gov/publications/ger\\_ms2012-02\\_geol\\_map\\_brinnon\\_24k.zip](http://www.dnr.wa.gov/publications/ger_ms2012-02_geol_map_brinnon_24k.zip)]
- Polenz, Michael; Wegmann, K. W.; Schasse, H. W., 2004, Geologic map of the Elwha and Angeles Point 7.5-minute quadrangles, Clallam County, Washington: Washington Division of Geology and Earth Resources Open File Report 2004-14, 1 sheet, scale 1:24,000 [[http://www.dnr.wa.gov/publications/ger\\_ofr2004-14\\_geol\\_map\\_elwha\\_angelespoint\\_24k.pdf](http://www.dnr.wa.gov/publications/ger_ofr2004-14_geol_map_elwha_angelespoint_24k.pdf)]

- Porter, S. C.; Carson, R. J., 1971, Problems of interpreting radiocarbon dates from dead-ice terrain, with an example from the Puget Lowland of Washington: *Quaternary Research*, v. 1, no. 3, p. 410-414.
- Porter, S. C.; Swanson, T. W., 1998, Radiocarbon age constraints on rates of advance and retreat of the Puget lobe of the Cordilleran ice sheet during the last glaciation: *Quaternary Research*, v. 50, no. 3, p. 205-213.
- Pratt, T. L.; Johnson, S. Y.; Potter, C. J.; Stephenson, W. J.; Finn, C. A., 1997, Seismic reflection images beneath Puget Sound, western Washington State—The Puget Lowland thrust sheet hypothesis: *Journal of Geophysical Research*, v. 102, no. B12, p. 27,469-27,489.
- Prescott, J. R.; Hutton, J. T., 1994, Cosmic ray contribution to dose rates for luminescence and ESR dating—Large depths and long-term time variations: *Radiation Measurements*, v. 23, no. 2-3, p. 497-500.
- Puget Sound Lidar Consortium, 2002, Thurston Co, Mason Co, Jefferson Co, Vashon Island, and Pierce Co. Peninsula [GIS raster data]. [<http://pugetsoundlidar.ess.washington.edu/>]
- Raisz, E. J., 1945, The Olympic–Wallowa lineament: *American Journal of Science*, v. 243A [Daly volume], p. 479-485. [<http://earth.geology.yale.edu/~ajs/1945A/479.pdf>]
- Rau, W. W., 1964, Foraminifera from the northern Olympic Peninsula, Washington: U.S. Geological Survey Professional Paper 374-G, 33 p., 7 plates. [<http://pubs.er.usgs.gov/usgspubs/pp/pp374G>]
- Rau, W. W., 1981, Pacific Northwest Tertiary benthic foraminiferal biostratigraphic framework—An overview. *In* Armentrout, J. M., editor, *Pacific Northwest Cenozoic biostratigraphy*: Geological Society of America Special Paper 184, p. 67-84.
- Rau, W. W., 2000, Appendix 4—Foraminifera from the Carlsborg 7.5-minute quadrangle, Washington. *In* Schasse, H. W.; Wegmann, K. W., *Geologic map of the Carlsborg 7.5-minute quadrangle, Clallam County, Washington*: Washington Division of Geology and Earth Resources Open File Report 2000-7, p. 24-26. [[http://www.dnr.wa.gov/publications/ger\\_ofr2000-7\\_geol\\_map\\_carlsborg\\_24k.zip](http://www.dnr.wa.gov/publications/ger_ofr2000-7_geol_map_carlsborg_24k.zip)]
- Rau, W. W., 2004, Pacific Northwest Tertiary foraminiferal collections of the U.S. Geological Survey and the State of Washington: Washington Division of Geology and Earth Resources Digital Report 4, 1 Excel file. [[http://www.dnr.wa.gov/publications/ger\\_dr4\\_pacific\\_nw\\_foram\\_collections.zip](http://www.dnr.wa.gov/publications/ger_dr4_pacific_nw_foram_collections.zip)]
- Rhodes, E. J., 2011, Optically stimulated luminescence dating of sediments over the past 200,000 years: *Annual Review of Earth and Planetary Sciences*, v. 39, p. 461-488.
- Rigg, G. B.; Gould, H. R., 1957, Age of Glacier Peak eruption and chronology of post-glacial peat deposits in Washington and surrounding areas: *American Journal of Science*, v. 255, no. 5, p. 341-363.
- Rigg, G. B., 1958, Peat Resources of Washington: Division of Mines and Geology, p. 66-67. [[http://www.dnr.wa.gov/publications/ger\\_b44\\_peat\\_reasources\\_wa\\_1.pdf](http://www.dnr.wa.gov/publications/ger_b44_peat_reasources_wa_1.pdf)]
- Schasse, H. W.; Kalk, M. L.; Petersen, B. B.; Polenz, Michael, 2009, Geologic map of the Langley and western part of the Tulalip 7.5-minute quadrangles, Island County, Washington: Washington Division of Geology and Earth Resources Geologic Map GM-69, 1 sheet, scale 1:24,000. [[http://www.dnr.wa.gov/publications/ger\\_gm69\\_geol\\_map\\_langley\\_24k.pdf](http://www.dnr.wa.gov/publications/ger_gm69_geol_map_langley_24k.pdf)]
- Schasse, H. W.; Logan, R. L., 1998, Geologic map of the Sequim 7.5-minute quadrangle, Clallam County, Washington: Washington Division of Geology and Earth Resources Open File Report 98-7, 2 sheets, scale 1:24,000, with 28 p. text [[http://www.dnr.wa.gov/publications/ger\\_ofr98-7\\_geol\\_map\\_sequim\\_24k.zip](http://www.dnr.wa.gov/publications/ger_ofr98-7_geol_map_sequim_24k.zip)]
- Schasse, H. W.; Polenz, Michael, 2002, Geologic map of the Morse Creek 7.5-minute quadrangle, Clallam County, Washington: Washington Division of Geology and Earth Resources Open File Report 2002-8, 2 sheets, scale 1:24,000, with 26 p. text [[http://www.dnr.wa.gov/publications/ger\\_ofr2002-8\\_geol\\_map\\_morsecreek\\_24k.zip](http://www.dnr.wa.gov/publications/ger_ofr2002-8_geol_map_morsecreek_24k.zip)]
- Schasse, H. W.; Slaughter, S. L., 2005, Geologic map of the Port Townsend South and part of the Port Townsend North 7.5-minute quadrangles, Jefferson County, Washington: Washington Division of Geology and Earth Resources Geologic Map 57, 1 sheet, scale 1:24,000 [[http://www.dnr.wa.gov/publications/ger\\_gm57\\_geol\\_map\\_porttownsends\\_24k.pdf](http://www.dnr.wa.gov/publications/ger_gm57_geol_map_porttownsends_24k.pdf)]
- Schasse, H. W.; Wegmann, K. W., 2000, Geologic map of the Carlsborg 7.5-minute quadrangle, Clallam County, Washington: Washington Division of Geology and Earth Resources Open File Report 2000-7, 2 sheets, scale 1:24,000, with 33 p. text [[http://www.dnr.wa.gov/publications/ger\\_ofr2000-7\\_geol\\_map\\_carlsborg\\_24k.zip](http://www.dnr.wa.gov/publications/ger_ofr2000-7_geol_map_carlsborg_24k.zip)]
- Schasse, H. W.; Wegmann, K. W.; Polenz, Michael, 2004, Geologic map of the Port Angeles and Ediz Hook 7.5-minute Quadrangles, Clallam County, Washington: Washington Division of Geology and Earth Resources Open File Report 2004-13, 1 sheet, scale 1:24,000 [[http://www.dnr.wa.gov/publications/ger\\_ofr2004-13\\_geol\\_map\\_portangeles\\_edizhook\\_24k.pdf](http://www.dnr.wa.gov/publications/ger_ofr2004-13_geol_map_portangeles_edizhook_24k.pdf)]
- Sherrod, B. L.; Blakely, R. J.; Weaver, C. S.; Kelsey, H. M.; Barnett, Elizabeth; Liberty, Lee; Meagher, K. L.; Pape, Kristin, 2008, Finding concealed active faults—Extending the southern Whidbey Island fault across the Puget Lowland, Washington: *Journal of Geophysical Research*, v. 113, B05313. [doi:10.1029/2007JB005060, 2008]

- Sherrod, Brian; Blakely, R. J.; Weaver, Craig; Kelsey, H. M.; Barnett, Elizabeth; Wells, Ray, 2005a, Holocene fault scarps and shallow magnetic anomalies along the southern Whidbey Island fault zone near Woodinville, Washington [abstract]: *Eos* (American Geophysical Union Transactions), v. 86, no. 52, p. F1438.
- Sherrod, B. L.; Blakely, R. J.; Weaver, Craig; Kelsey, Harvey; Barnett, Elizabeth; Wells, Ray, 2005b, Holocene fault scarps and shallow magnetic anomalies along the southern Whidbey Island fault zone near Woodinville, Washington: U.S. Geological Survey Open-File Report 2005-1136, 35 p. [<http://pubs.usgs.gov/of/2005/1136/>]
- Simonds, F. W.; Longpre, C. I.; Justin, G. B., 2004, Ground-water system in the Chimacum Creek basin and surface water/ground water interaction in Chimacum and Tarboo Creeks and the Big and Little Quilcene Rivers, eastern Jefferson County, Washington: U.S. Geological Survey Scientific Investigations Report 2004-5058, 1 sheet, scale 1:31,680, 49 p. text. [<http://pubs.water.usgs.gov/sir2004-5058>]
- Snively, P. D., Jr., 1983, Day 1—Peripheral rocks—Tertiary geology of the northwestern part of the Olympic Peninsula, Washington. In Muller, J. E.; Snively, P. D., Jr.; Tabor, R. W., The Tertiary Olympic terrane, southwest Vancouver Island and northwest Washington: Geological Association of Canada Victoria Section Field Trip 12, p. 6-31
- Snively, P. D., Jr.; Niem, A. R.; Pearl, J. E., 1978, Twin River Group (upper Eocene to lower Miocene): Defined to include the Hoko River, Makah, and Pysht Formations, Clallam County, Washington. In Sohl, N. F.; Wright, W. B., Changes in stratigraphic nomenclature by the U.S. Geological Survey, 1977: U.S. Geological Survey Bulletin 1457-A, p. 111-120.
- Spencer, P. K., 1983, Depositional environment of some Eocene strata near Quilcene, Washington, based on trace-, macro-, and micro-fossils and lithologic associations. In Larue, D. K.; Steel, R. J., editors, Cenozoic marine sedimentation; Pacific margin, U.S.A.: Society of Economic Paleontologists and Mineralogists Pacific Section, p. 233-239.
- Spencer, P. K., 1984, Lower Tertiary biostratigraphy and paleoecology of the Quilcene–Discovery Bay area, northeast Olympic Peninsula, Washington: University of Washington Doctor of Philosophy thesis, 173 p., 2 plates.
- Squires, R. L.; Goedert, J. L.; Kaler, K. L., 1992, Paleontology and stratigraphy of Eocene rocks at Pulali Point, Jefferson County, eastern Olympic Peninsula, Washington: Washington Division of Geology and Earth Resources Report of Investigations 31, 27 p. [[http://www.dnr.wa.gov/publications/ger\\_ri31\\_eocene\\_rock\\_jefferson\\_county.pdf](http://www.dnr.wa.gov/publications/ger_ri31_eocene_rock_jefferson_county.pdf)]
- Tabor, R. W.; Cady, W. M., 1978, Geologic map of the Olympic Peninsula, Washington: U.S. Geological Survey Miscellaneous Investigations Series Map I-994, 2 sheets, scale 1:125,000. [<http://pubs.er.usgs.gov/publication/i994>]
- Tabor, R. W.; Haessler, P. J.; Haugerud, R. A.; Wells, R. E., 2011, Lidar-revised geologic map of the Uncas 7.5' quadrangle, Clallam and Jefferson Counties, Washington: U.S. Geological Survey Scientific Investigations Map: 3160, 1 sheet, scale 1:24,000 with 13 p. text. [<http://pubs.usgs.gov/sim/3160/>]
- Tepper, J. H.; Clark, Kenneth; Asmerom, Yemane; McIntosh, William, 2004, Eocene adakites in the Cascadia forearc—Implications for the position of the Kula–Farallon ridge [abstract]: Geological Society of America Abstracts with Programs, v. 36, no. 6, p. 69.
- Thorson, R. M., 1980, Ice-sheet glaciation of the Puget Lowland, Washington, during the Vashon Stade (late Pleistocene): *Quaternary Research*, v. 13, no. 3, p. 303-321.
- Thorson, R. M., 1981, Isostatic effects of the last glaciation in the Puget Lowland, Washington: U.S. Geological Survey Open-File Report 81-370, 100 p., 1 plate. [<http://pubs.er.usgs.gov/publication/ofr81370>]
- Thorson, R. M., 1989, Glacio-isostatic response of the Puget Sound area, Washington: *Geological Society of America Bulletin*, v. 101, no. 9, p. 1163-1174.
- Troost, K. G.; Booth, D. B., 2008, Geology of Seattle and the Seattle area, Washington. In Baum, R. L.; Godt, J. W.; Highland, L. M., editors, Landslides and engineering geology of the Seattle, Washington, area: Geological Society of America Reviews in Engineering Geology XX, p. 1-35. [[http://www.wou.edu/las/phyci/taylor/g473/seismic\\_hazards/troost\\_booth\\_2008\\_geo\\_seattle.pdf](http://www.wou.edu/las/phyci/taylor/g473/seismic_hazards/troost_booth_2008_geo_seattle.pdf)]
- U.S. Coast & Geodetic Survey, 1870 “T-sheet” coastal survey (register no. 1126). [<http://riverhistory.ess.washington.edu/tsheets/framedex.htm>]
- U.S. Department of Agriculture, Natural Resource Conservation Service, 2009, Web Soil Survey, status 9/22/2009 [GIS data]. [accessed Sept. 14, 2011, at <http://websoilsurvey.nrcs.usda.gov/>]
- U.S. Geological Survey Geologic Names Committee, 2010, Divisions of geologic time—Major chronostratigraphic and geochronologic units: U.S. Geological Survey Fact Sheet 2010-3059, 2 p. [<http://pubs.usgs.gov/fs/2010/3059/>]
- Waite, R. B., Jr.; Thorson, R. M., 1983, The Cordilleran ice sheet in Washington, Idaho, and Montana. In Porter, S. C., editor, The late Pleistocene; Volume 1 of Wright, H. E., Jr., editor, Late-Quaternary environments of the United States: University of Minnesota Press, p. 53-70.
- Walsh, T. J.; Korosec, M. A.; Phillips, W. M.; Logan, R. L.; Schasse, H. W., 1987, Geologic map of Washington--Southwest quadrant: Washington Division of Geology and Earth Resources Geologic Map GM-34, 2 sheets, scale 1:250,000, with 28 p. text. [[http://www.dnr.wa.gov/publications/ger\\_gm34\\_geol\\_map\\_sw\\_wa\\_250k.pdf](http://www.dnr.wa.gov/publications/ger_gm34_geol_map_sw_wa_250k.pdf)]

- Walsh, T. J.; Logan, R. L.; Polenz, Michael; Schasse, H. W., 2003, Geologic map of the Nisqually 7.5-minute quadrangle, Thurston and Pierce Counties, Washington: Washington Division of Geology and Earth Resources Open File Report 2003-10, 1 sheet, scale 1:24,000. [[http://www.dnr.wa.gov/publications/ger\\_ofr2003-10\\_geol\\_map\\_nisqually\\_24k.pdf](http://www.dnr.wa.gov/publications/ger_ofr2003-10_geol_map_nisqually_24k.pdf)]
- Weaver, C. E., 1937, Tertiary stratigraphy of western Washington and northwestern Oregon: University of Washington Publications in Geology, v. 4, 266 p.
- Whetten, J. T.; Carroll, P. I.; Gower, H. D.; Brown, E. H.; Pessl, Fred, Jr., 1988, Bedrock geologic map of the Port Townsend 30-by 60-minute quadrangle, Puget Sound region, Washington: U.S. Geological Survey Miscellaneous Investigations Series Map I-1198-G, 1 sheet, scale 1:100,000. [<http://pubs.er.usgs.gov/publication/i1198G>]
- Wolfe, E. W.; McKee, E. H., 1972, Sedimentary and igneous rocks of the Grays River quadrangle, Washington: U.S. Geological Survey Bulletin 1335, 70 p. [<http://pubs.er.usgs.gov/usgspubs/b/b1335>]
- Wolfe, M. R.; Tepper, J. H., 2004, Felsic Eocene volcanic rocks on the Olympic Peninsula and their implications for ridge subduction [abstract]: Geological Society of America Abstracts with Programs, v. 36, no. 5, p. 223.
- Yount, J. C.; Gower, H. D., 1991, Bedrock geologic map of the Seattle 30' by 60' quadrangle, Washington: U.S. Geological Survey Open-File Report 91-147, 37 p., 4 plates. [<http://pubs.er.usgs.gov/publication/ofr91147>]
- Yount, J. C.; Minard, J. P.; Dembroff, G. R., 1993, Geologic map of surficial deposits in the Seattle 30' x 60' quadrangle, Washington: U.S. Geological Survey Open-File Report 93-233, 2 sheets, scale 1:100,000. [[http://ngmdb.usgs.gov/Prodesc/proddesc\\_12654.htm](http://ngmdb.usgs.gov/Prodesc/proddesc_12654.htm)]

## Appendix A. New Radiocarbon and Luminescence Age Estimates

**Table A1.** Radiocarbon age-control data from the map area. Analysis performed by Beta Analytic, Inc. Site is shown as age site GD1 on map sheet. Latitude and longitude coordinates were generated from sample locations as plotted in ArcGIS (projection Washington State Plane South, NAD 83 HARN, U.S. Survey feet). Elevation is in feet, estimated using Puget Sound Lidar Consortium lidar (vertical datum NAVD88, projected to Washington State Plane South, NAD 83 HARN, U.S. Survey feet) supplemented by visual elevation estimate. The lidar-based statement was not adjusted to account for projection differences relative to the base map (vertical datum NGVD 29)—lidar level 0 theoretically is 3.52 to 3.64 ft below base map level 0 [[http://www.ngs.noaa.gov/cgi-bin/VERTCON/vert\\_con.prj](http://www.ngs.noaa.gov/cgi-bin/VERTCON/vert_con.prj)]. Geologic unit is the interpretation of this study for the sample host material. Age estimate in radiocarbon years before 1950 ( $^{14}\text{C}$  yr BP) is reported with one standard deviation of uncertainty ( $1\sigma = 68\%$  confidence interval) and is "conventional" (adjusted for measured  $^{13}\text{C}/^{12}\text{C}$  ratio). Age estimate stated in ka is in calendar years before 1950 divided by 1,000 and is reported with two standard deviations of uncertainty ( $2\sigma = 95\%$  confidence interval) as reported by Beta Analytic, Inc. Uncertainty statement reflects random and lab errors; errors from unrecognized sample characteristics or flawed methodological assumptions (for example,  $^{14}\text{C}$  sample contamination from younger carbon flux) is not known.

Age site	Field/Lab sample ID	TRS	Lat/long (degrees)	Elev. (ft)	Map unit	Material dated	Analytic method	$^{13}\text{C}/^{12}\text{C}$ (o/oo)	Age estimate	Notes
GD1	M166a/Beta 365739	sec. 4, T28N R1W	47.940734-122.818106	274	Qgaf	plant fragment	$^{14}\text{C}$ (AMS)	-21.7	14,880 $\pm$ 60 $^{14}\text{C}$ yr BP (18.470–18.300 and 18.090–17.960 ka)	Delicate detrital fragment of a terrestrial or aquatic plant, most likely a graminoid (grass or sedge) or other monocot, such as eelgrass ( <i>Zostera</i> sp), ditchgrass ( <i>Ruppia</i> sp.?), <i>Potamogeton</i> sp., or sedge ( <i>Carex</i> sp.). Sampled from a horizontally laminated silt exposure with isolated east-southeast-directed, gentle paleocurrent indications (climbing ripples). (Sampled 11 ft above Chimacum Creek, 6 ft below top of a 10-ft-high by 100-ft-wide south-side cutbank exposure). Compaction and upsection Vashon deposits confirm that the deposit is older than Vashon Till. Field relations suggest a stratigraphic position below age sites GD2, GD3, and GD4.

**Table A2.** Infrared and optically stimulated luminescence age-control results from the map area. All dates are new. Optically stimulated luminescence (OSL) analysis and infrared stimulated luminescence (IRSL) analysis performed by Shannon Mahan, USGS. Analytical data are provided in Table A3. Sites are shown on the map sheet. Uncertainty values of age estimates span one standard deviation ( $1\sigma = 68\%$  confidence interval). Uncertainty statements reflect random and lab errors; errors from unrecognized sample characteristics or flawed methodological assumptions (for example, incomplete pre-depositional re-setting of luminescence samples) are not known.

Age site	Field/Lab sample ID	TRS	Lat/long (degrees)	Elev. (ft)	Map unit	Material dated	Analytic method	Age estimate	Notes
GD2	M707	sec. 23, T29N R1W	47.993873 -122.764883	280	Qgas	sand	OSL	15,760 ±1,180 ka	Compact, pale gray, clean and well sorted, rhythmically bedded, fine-medium sand and silty sand, likely lacustrine. Sand mineralogy in thin section is dominantly quartz (30%), polycrystalline quartz (10–15%), plagioclase feldspar (2–3%), potassium feldspar (1–2%), lithics (1–2%), and rare altered basalts, mudstones and a few chert clasts. Remaining ~60% of thin section is mounting resin in section produced from loose, single grained sand sample. Beds are parallel and horizontally planar rhythmites within a 2 ft <sup>2</sup> hole (hand-dug beneath the base of a 6.5 ft-deep, fresh bulldozer cut). Rhythmites consist of about 1 mm-thick, dark gray laminae alternating with 1–4 mm-thick, pale gray laminae. Multiple pale orange brown, iron-stained zones are each less than 4 cm thick and include both lighter and darker beds.
							IRSL	17,060 ±1,040 ka	
GD3	M563	sec. 5, T28N R1W	47.945428 -122.826514	355	Qgas	sand	OSL	11,810 ±1,010 ka	Compact, approximately horizontally bedded to gently cross bedded and cross laminated, micaceous sand and silt (dominantly medium sand to silt, ranges to granule sand). Sand fraction in thin section is well sorted, equigranular, angular to subrounded. Major minerals include quartz (40–50%), polycrystalline quartz (10–15%), amphibole (5–7%). Remaining ~55% of thin section is mounting resin in section produced from loose, single grained sand sample. A single mudstone or basalt pebble is embedded in the exposure. Beds suggest a low-energy current setting. Paleocurrent indicators favor south- or southeast-directed currents but permit currents between south- and west-directed.
							IRSL	19,260 ±1,390 ka	
GD4	M735B	sec. 15, T28N R1W	47.924860 -122.796445	456	Qga	sand	OSL	16,540 ±1,510 ka	Compact, pale gray and dry, medium sand. Extremely well-sorted and clean. Sand mineralogy is quartz (15%), polycrystalline quartz (7%), potassium feldspar (3–5%), opaque minerals (3–5%), unknown minerals (3–5%), plagioclase feldspar (1–2%), and amphiboles (1–2%). Remaining ~60 to 70 percent of thin section is mounting resin in section produced from loose, single grained sand sample. Bedding ranges from horizontal and planar to broadly and gently channel cross bedded. High-grade metamorphic clasts abound in isolated pebbly lenses and indicate a northern (proglacial) source. Exposure suggests a large channel setting.
							IRSL	84,430 ±4,970 ka	

**Table A3.** Luminescence analytical data for age-control results from the map area. This table provides elemental concentrations, cosmic and total dose rates, equivalent doses, and ages from IRSL (fine-grained feldspars) and OSL (quartz). Detailed sample descriptions are provided in Table A2. For field moisture content, values in parentheses indicate the complete sample saturation in percent. Ages calculated using approximately 55 percent of saturation values. Analyses of potassium (K), uranium (U), and thorium (Th) obtained using high-resolution gamma spectrometry (HPGe detector). Cosmic doses and attenuation with depth were calculated using methods of Prescott and Hutton (1994). The unit of absorbed radiation is Grays (Gy). Number (n) is the number of replicated equivalent dose (De) estimates used to calculate the equivalent dose. Values in parentheses indicate total number of measurements included in calculating the represented equivalent dose and age using the minimum age model (MAM). All aliquots passed methodology tests, except M707, which had many "dim" quartz aliquots. Dose rate and OSL age for quartz are from fine (250–180 micron) quartz. Linear + exponential fit was used on equivalent doses, with single aliquot regeneration; errors are to one sigma; ages and errors are rounded. Dose rate and IRSL age for feldspar from fine (4–11 micron) polymineral silt. Exponential fit used for multiple aliquot additive doses. Errors are to one sigma. Fade tests indicate ~1 g/decade correction.

Age site	Field/lab sample ID	Water content (%)	K (%)	U (ppm)	Th (ppm)	Cosmic dose additions (Gy/ka)	Equivalent dose (Gy)	Total dose rate (Gy/ka)	n	Analytic method	Age estimate
GD2	M707	8 (22)	1.12 ±0.05	1.25 ±0.15	6.05 ±0.43	0.17 ±0.01	29.0 ±1.68	1.84 ±0.09	9 (30)	OSL	15.760 ±1.180 ka
							44.7 ±1.70	2.62 ±0.13			IRSL
GD3	M563	9 (24)	0.95 ±0.03	0.80 ±0.14	3.39 ±0.39	0.18 ±0.01	16.5 ±0.89	1.40 ±0.10	17 (30)	OSL	11.810 ±1.010 ka
							36.2 ±0.87	1.88 ±0.13			IRSL
GD4	M735B	6 (19)	1.15 ±0.02	0.92 ±0.08	2.29 ±0.19	0.18 ±0.01	25.8 ±2.14	1.56 ±0.06	12 (24)	OSL	16.540 ±1.510 ka
							171 ±7.71	2.03 ±0.08			IRSL

## Appendix B. Crustal Earthquake Data

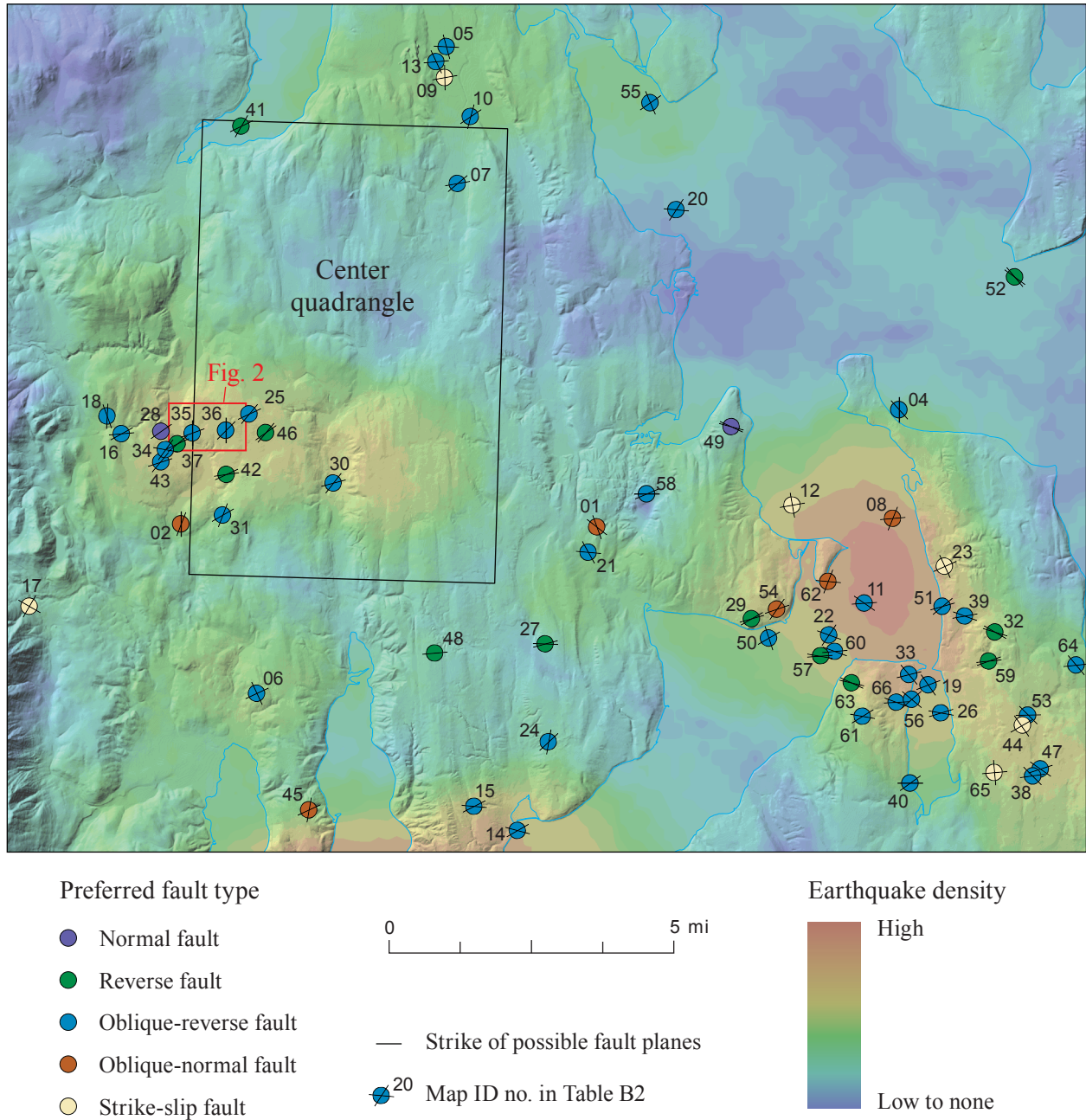


**Figure B1.** Locations of earthquakes and focal mechanisms near the Center quadrangle (outlined in black). Hillshade image color shading symbolizes earthquake epicentral density based on all 738 recorded crustal earthquakes (1970–2014)(www.pnsn.org); the color scale is relative (i.e., “high” is high for this area, and “low” low for this area, with no comparison to event densities elsewhere). Surface events were assumed to be mining activity and were ignored for the purposes of this study. Numbers correspond to “Map ID no.” in Table B2, which provides complete earthquake parameters and focal mechanisms for the 66 events. All but two events are deeper than 13 km. Of the 14 events near the southwest map corner, nine are oblique-reverse (includes two oblique-reverse strike-slip events), three are reverse, one is normal, and one oblique-normal and shallow. The single event beneath the northwest map corner is reverse and occurred at a depth of 21.3 km.

**Table B2.** Crustal earthquakes with focal mechanisms in and near the map area. Recorded crustal seismic events (earthquakes) as reported by PNSN ([www.pnsn.org](http://www.pnsn.org)) for 1970 to 2014 (accessed March 5, 2014). Figure B1 shows the events by their spatial distribution, type of movement, and possible azimuthal strike orientations. (Map ID no. 3 not shown because it is outside the figure area.) Strike, dip, and rake options 1 and 2 define the two sets of possible focal mechanisms for each event. (Focal mechanism analysis does not favor either set of solutions.) All but two of the 66 events occurred in the lower crust between 13 and 28 km. (We excluded events below 44 km on the assumption that those are subduction related). Focal mechanisms are illustrated using the RFOC package (Lees, 2007) prepared in the computing language R (<http://cran.us.r-project.org/>).

Map ID no.	Latitude and longitude (decimal degrees)	Depth (km)	Magnitude	Strike (°) (option 1)	Dip (°) (option 1)	Rake (°) (option 1)	Strike (°) (option 2)	Dip (°) (option 2)	Rake (°) (option 2)	Preferred fault type	Focal mechanism illustration	Hyperlink
1	47.8902 -122.719	0	1.5	160	55	-70	308	40	-116	oblique-normal		<a href="http://www.pnsn.org/event/60441267">http://www.pnsn.org/event/60441267</a>
2	47.8877 -122.889	6.9	0.9	0	15	-110	201	76	-85	oblique-normal		<a href="http://www.pnsn.org/event/60563591">http://www.pnsn.org/event/60563591</a>
3	48.053 -122.962	13.3	2.4	35	55	110	183	40	64	oblique-reverse		<a href="http://www.pnsn.org/event/10269243">http://www.pnsn.org/event/10269243</a>
4	47.9247 -122.597	13.7	1.8	0	50	120	138	48	59	oblique-reverse		<a href="http://www.pnsn.org/event/10434573">http://www.pnsn.org/event/10434573</a>
5	48.021 -122.787	15.4	1.1	165	25	160	273	82	66	oblique-reverse strike-slip		<a href="http://www.pnsn.org/event/60505871">http://www.pnsn.org/event/60505871</a>
6	47.8418 -122.856	15.6	0.6	65	90	40	335	50	180	oblique-reverse strike-slip		<a href="http://www.pnsn.org/event/60438942">http://www.pnsn.org/event/60438942</a>
7	47.9835 -122.78	16	2.6	80	50	110	230	44	67	oblique-reverse		<a href="http://www.pnsn.org/event/10268123">http://www.pnsn.org/event/10268123</a>
8	47.8948 -122.599	16.6	2	85	65	-50	202	46	-144	oblique-normal		<a href="http://www.pnsn.org/event/10511718">http://www.pnsn.org/event/10511718</a>
9	48.0125 -122.787	17	1.1	80	25	-10	179	86	-115	strike-slip		<a href="http://www.pnsn.org/event/60505866">http://www.pnsn.org/event/60505866</a>
10	48.002 -122.776	17.4	1	15	65	70	236	32	126	oblique-reverse		<a href="http://www.pnsn.org/event/60408561">http://www.pnsn.org/event/60408561</a>
11	47.8713 -122.609	17.5	1.9	125	45	120	266	52	64	oblique-reverse		<a href="http://www.pnsn.org/event/10426623">http://www.pnsn.org/event/10426623</a>
12	47.8977 -122.64	17.5	2.7	80	90	-10	170	80	180	strike-slip		<a href="http://www.pnsn.org/event/10245758">http://www.pnsn.org/event/10245758</a>
13	48.0168 -122.791	17.6	1.8	85	50	30	335	67	136	oblique-reverse strike-slip		<a href="http://www.pnsn.org/event/60503806">http://www.pnsn.org/event/60503806</a>
14	47.8062 -122.748	17.6	3	105	55	120	240	45	55	oblique-reverse		<a href="http://www.pnsn.org/event/10487483">http://www.pnsn.org/event/10487483</a>
15	47.8125 -122.766	17.8	1.6	95	55	110	243	40	64	oblique-reverse		<a href="http://www.pnsn.org/event/10829093">http://www.pnsn.org/event/10829093</a>
16	47.912 -122.915	18.1	2.2	85	35	110	241	57	77	oblique-reverse		<a href="http://www.pnsn.org/event/10859373">http://www.pnsn.org/event/10859373</a>

Map ID no.	Latitude and longitude (decimal degrees)	Depth (km)	Magnitude	Strike (°) (option 1)	Dip (°) (option 1)	Rake (°) (option 1)	Strike (°) (option 2)	Dip (°) (option 2)	Rake (°) (option 2)	Preferred fault type	Focal mechanism illustration	Hyperlink
17	47.8638 -122.95	18.2	2.5	120	45	180	30	90	-45	strike-slip		<a href="http://www.pnsn.org/event/10606843">http://www.pnsn.org/event/10606843</a>
18	47.9167 -122.921	18.3	0.8	160	30	70	3	62	101	oblique-reverse		<a href="http://www.pnsn.org/event/60381821">http://www.pnsn.org/event/60381821</a>
19	47.8493 -122.582	18.4	1.6	145	65	150	249	63	28	oblique-reverse strike-slip		<a href="http://www.pnsn.org/event/10442758">http://www.pnsn.org/event/10442758</a>
20	47.978- 122.691	18.7	2.7	95	25	150	213	78	68	oblique-reverse strike-slip		<a href="http://www.pnsn.org/event/10153443">http://www.pnsn.org/event/10153443</a>
21	47.8832 -122.723	19.2	2	95	55	50	331	51	133	oblique-reverse		<a href="http://www.pnsn.org/event/10721488">http://www.pnsn.org/event/10721488</a>
22	47.8623 -122.623	19.4	2.3	110	65	150	214	63	28	oblique-reverse strike-slip		<a href="http://www.pnsn.org/event/10845668">http://www.pnsn.org/event/10845668</a>
23	47.882 -122.577	19.6	1.9	335	85	170	66	80	5	strike-slip		<a href="http://www.pnsn.org/event/10527383">http://www.pnsn.org/event/10527383</a>
24	47.8308 -122.737	19.7	1.3	10	40	60	227	56	113	oblique-reverse		<a href="http://www.pnsn.org/event/60548516">http://www.pnsn.org/event/60548516</a>
25	47.9185 -122.863	19.7	2.2	40	40	70	245	53	106	oblique-reverse		<a href="http://www.pnsn.org/event/10225108">http://www.pnsn.org/event/10225108</a>
26	47.8417 -122.577	19.7	2.7	100	45	110	253	48	71	oblique-reverse		<a href="http://www.pnsn.org/event/10207728">http://www.pnsn.org/event/10207728</a>
27	47.8577 -122.739	19.9	1.6	75	55	80	272	36	104	reverse		<a href="http://www.pnsn.org/event/10805208">http://www.pnsn.org/event/10805208</a>
28	47.913 -122.899	20	0.9	55	70	-90	235	20	-90	normal		<a href="http://www.pnsn.org/event/60558687">http://www.pnsn.org/event/60558687</a>
29	47.8662 -122.655	20	2.2	60	45	80	254	46	100	reverse		<a href="http://www.pnsn.org/event/10781103">http://www.pnsn.org/event/10781103</a>
30	47.9002- 122.828	20	2	75	40	120	218	56	67	oblique-reverse		<a href="http://www.pnsn.org/event/10569128">http://www.pnsn.org/event/10569128</a>
31	47.8905 -122.872	20	2.8	60	45	120	201	52	64	oblique-reverse		<a href="http://www.pnsn.org/event/10198863">http://www.pnsn.org/event/10198863</a>
32	47.8643 -122.556	20.1	2.1	120	40	100	287	51	82	reverse		<a href="http://www.pnsn.org/event/10409048">http://www.pnsn.org/event/10409048</a>
33	47.852 -122.59	20.3	1.9	140	55	140	256	58	43	oblique-reverse strike-slip		<a href="http://www.pnsn.org/event/10289378">http://www.pnsn.org/event/10289378</a>
34	47.908 -122.897	20.7	1.8	100	55	140	216	58	43	oblique-reverse strike-slip		<a href="http://www.pnsn.org/event/10801283">http://www.pnsn.org/event/10801283</a>

Map ID no.	Latitude and longitude (decimal degrees)	Depth (km)	Magnitude	Strike (°) (option 1)	Dip (°) (option 1)	Rake (°) (option 1)	Strike (°) (option 2)	Dip (°) (option 2)	Rake (°) (option 2)	Preferred fault type	Focal mechanism illustration	Hyperlink
35	47.9128 -122.886	20.8	1.7	70	65	139	180	54	32	oblique-reverse strike-slip		<a href="http://www.pnsn.org/event/10832248">http://www.pnsn.org/event/10832248</a>
36	47.9138 -122.872	20.9	1.5	0	55	60	225	45	125	oblique-reverse		<a href="http://www.pnsn.org/event/10807108">http://www.pnsn.org/event/10807108</a>
37	47.9097 -122.892	20.9	1.3	50	50	80	245	41	101	reverse		<a href="http://www.pnsn.org/event/10802168">http://www.pnsn.org/event/10802168</a>
38	47.8248 -122.536	21	2.2	135	50	130	262	54	52	oblique-reverse		<a href="http://www.pnsn.org/event/10186623">http://www.pnsn.org/event/10186623</a>
39	47.8685 -122.568	21.1	2	80	50	70	290	44	113	oblique-reverse		<a href="http://www.pnsn.org/event/10347658">http://www.pnsn.org/event/10347658</a>
40	47.8222- 122.589	21.2	1.9	90	60	110	234	36	59	oblique-reverse		<a href="http://www.pnsn.org/event/10236963">http://www.pnsn.org/event/10236963</a>
41	47.9975 -122.87	21.3	1.6	30	75	80	244	18	123	reverse		<a href="http://www.pnsn.org/event/10753158">http://www.pnsn.org/event/10753158</a>
42	47.9017 -122.871	21.3	3.3	65	55	80	262	36	104	reverse		<a href="http://www.pnsn.org/event/10187263">http://www.pnsn.org/event/10187263</a>
43	47.905 -122.898	21.4	1.7	40	55	70	252	40	116	oblique-reverse		<a href="http://www.pnsn.org/event/10795133">http://www.pnsn.org/event/10795133</a>
44	47.84 -122.543	21.6	1.3	60	60	10	325	81	150	strike-slip		<a href="http://www.pnsn.org/event/60532032">http://www.pnsn.org/event/60532032</a>
45	47.8102 -122.834	21.6	0.6	65	35	-40	190	68	-118	oblique-normal strike-slip		<a href="http://www.pnsn.org/event/60393511">http://www.pnsn.org/event/60393511</a>
46	47.9135 -122.856	21.7	1.6	40	50	80	235	41	101	reverse		<a href="http://www.pnsn.org/event/10806673">http://www.pnsn.org/event/10806673</a>
47	47.827 -122.536	22	2.8	125	50	130	252	54	52	oblique-reverse		<a href="http://www.pnsn.org/event/10186403">http://www.pnsn.org/event/10186403</a>
48	47.8543 -122.784	22.4	2.1	85	65	90	265	25	90	reverse		<a href="http://www.pnsn.org/event/10686673">http://www.pnsn.org/event/10686673</a>
49	47.9188 -122.666	22.6	1.4	105	15	-100	295	75	-87	normal		<a href="http://www.pnsn.org/event/60589052">http://www.pnsn.org/event/60589052</a>
50	47.861- 122.648	22.8	1.3	60	75	140	162	52	19	oblique-reverse strike-slip		<a href="http://www.pnsn.org/event/60403736">http://www.pnsn.org/event/60403736</a>
51	47.871 -122.577	22.8	2.6	50	35	70	254	57	103	oblique-reverse		<a href="http://www.pnsn.org/event/10159558">http://www.pnsn.org/event/10159558</a>
52	47.962 -122.551	23.4	2.8	140	45	100	306	46	80	reverse		<a href="http://www.pnsn.org/event/10857333">http://www.pnsn.org/event/10857333</a>

Map ID no.	Latitude and longitude (decimal degrees)	Depth (km)	Magnitude	Strike (°) (option 1)	Dip (°) (option 1)	Rake (°) (option 1)	Strike (°) (option 2)	Dip (°) (option 2)	Rake (°) (option 2)	Preferred fault type	Focal mechanism illustration	Hyperlink
53	47.841 -122.542	23.7	1.9	135	35	130	269	64	66	oblique-reverse		<a href="http://www.pnsn.org/event/10664378">http://www.pnsn.org/event/10664378</a>
54	47.869 -122.645	24	0.8	35	60	-110	251	36	-59	oblique-normal		<a href="http://www.pnsn.org/event/60394587">http://www.pnsn.org/event/60394587</a>
55	48.0072 -122.702	24.1	1.8	55	55	160	157	74	37	oblique-reverse strike-slip		<a href="http://www.pnsn.org/event/10813878">http://www.pnsn.org/event/10813878</a>
56	47.8452 -122.589	24.4	1.3	130	65	160	229	72	26	oblique-reverse strike-slip		<a href="http://www.pnsn.org/event/10530413">http://www.pnsn.org/event/10530413</a>
57	47.8572 -122.625	24.5	1.9	100	45	100	266	46	80	reverse		<a href="http://www.pnsn.org/event/60421367">http://www.pnsn.org/event/60421367</a>
58	47.8997 -122.699	24.9	2.2	90	30	110	247	62	79	oblique-reverse		<a href="http://www.pnsn.org/event/10691768">http://www.pnsn.org/event/10691768</a>
59	47.8563 -122.558	25	2.3	70	45	80	264	46	100	reverse		<a href="http://www.pnsn.org/event/10206043">http://www.pnsn.org/event/10206043</a>
60	47.8572- 122.621	25.4	2.4	85	40	70	290	53	106	oblique-reverse		<a href="http://www.pnsn.org/event/10735233">http://www.pnsn.org/event/10735233</a>
61	47.8402 -122.609	25.7	3.2	100	50	120	238	48	59	oblique-reverse		<a href="http://www.pnsn.org/event/10766178">http://www.pnsn.org/event/10766178</a>
62	47.877 -122.624	25.8	1.6	95	60	-30	201	64	-146	oblique-normal strike-slip		<a href="http://www.pnsn.org/event/60438872">http://www.pnsn.org/event/60438872</a>
63	47.8493 -122.614	25.8	2.2	115	35	100	283	56	83	reverse		<a href="http://www.pnsn.org/event/10735288">http://www.pnsn.org/event/10735288</a>
64	47.8558 -122.522	26.4	2.4	140	55	130	264	51	47	oblique-reverse		<a href="http://www.pnsn.org/event/10656848">http://www.pnsn.org/event/10656848</a>
65	47.8257 -122.554	27	2.3	355	90	-170	265	80	0	strike-slip		<a href="http://www.pnsn.org/event/10812338">http://www.pnsn.org/event/10812338</a>
66	47.8443 -122.595	27.5	2.1	110	30	110	267	62	79	oblique-reverse		<a href="http://www.pnsn.org/event/10710318">http://www.pnsn.org/event/10710318</a>